EFFECT OF SHIELD SPLITTING AND PLACEMENT IN NUCLEAR PROPELLED SPACE VEHICLES

Final Report under Contract NASW-132
TRG-136-FR

Authors:

Raphael Aronson
Raphael Aronson

Carl N Klahr
Carl N. Klahr

Herbert Steinberg
Herbert Steinberg

Kalman Held
Kalman Held

Submitted to:

National Aeronautics & Space Administration
Washington 25, D. C.

Submitted by:
TRG, Incorporated
2 Aerial Way
Syosset, New York

March 1, 1961

TECHNICAL RESEARCH GROUP

ACKNOWLEDGEMENTS

Acknowledgements are due to Dr. Martin Kelly for his help with a preliminary analytical approach to the problem and to Dr. Leonard Solon for many helpful discussions. Thanks are due also to Mrs. Patience Darrow, who had the arduous task of typing this report.

ABSTRACT

The effect of splitting and placement of various idealized shadow shield configurations appropriate to manned nuclear rockets has been investigated. The effect on neutron dose in both hydrogenous and nonhydrogenous shield situations was considered, as well as the effect on gamma dose. The results indicate that in some circumstances proper placement or multiple splitting of the shield can affect the dose by a factor of three or more, over and above any r^2 effect due to differences in the relative sizes of reactor and payload.

TABLE OF CONTENTS

Section No.		Page No.
1.	Introduction and Summary	1
2.	Shielding Requirements for Nuclear Rocket Propulsion	4
3.	Qualitative Discussion of Shield Splitting and Placement	11
4.	Monte Carlo Calculation Results and Conclusions	21
4.1	Description of Calculations	24
4.2	Results of Monte Carlo Calculations	35
	References	A.78

List of Appendices

Appendix No.		Page No.
1	Description of Monte Carlo Codes	A.1
2	Sampling Procedure	A.25
3	Generalized Quota Sampling	A.36
4.	Operating Instructions for Monte Carlo Code	A.43
5.	Flow Sheets for Monte Carlo Calculations ..	A.62

List of Illustrations

Figure No.		Page No.
1.	Illustrative Shield Configurations	A.2
2.	Typical Geometry at Collision	A.8

List of Tables

Table No.		Page No.
1.	Required Number of Attenuation Lengths	10
1a.	Typical Attenuation Coefficients for Neutrons and Gammas	10
2.	Shield Splitting Improvement Factor-Analytical Formulas	14
3.	Shield Geometries and Materials-Gamma Rays	31
4.	Shield Geometries and Materials-Neutrons	32-34
5.	Gamma Ray Fluxes for Various Shield Configurations	43-44
6.	Neutron Fluxes for Various Shield Configurations	45-53
7.	Comparative Doses for Hydrogen Shields 2.5 Ft. Thick	35
8.	Shield Component Table for Code for Input Block 2 (Gamma Rays)	A.47
9.	Element Table for Code for Input Block 2 (Neutrons).....	A.47
10.	Wavelength and Energy Arguments for Cross Section Tables for Gamma Ray Code	A.50
11.	Energy Arguments for Cross Section Tables for Neutron Code	A.51
12.	Error Indicator Names	A.58
13.	Error Printout Data	A.59-A.60

Section 1. Introduction and Summary

This report is concerned with a study of shielding principles for nuclear reactors in space vehicles. In particular, the concept: of multiple splitting of the shield and of optimal shield placement have been investigated. In the course of this investigation analytical and numerical calculation methods have been developed for the evaluation of nuclear reactor shields in space.

The important difference between space shielding and conventional shielding problems is the absence of a scattering atmosphere. This makes it unnecessary to shield the payload (the detector or the crew) from atmosphere-scattered radiation. Radiation which diverges from the line-of-sight path or cone-of-sight path from source to detector may be regarded as lost. Thus th shield should be a shadow shield. The possibility then arises of eliminating much of the penetrating radiation by scattering it into space, since a deviation from the cone-of-sight is equivalent to an absorption. This is quite different than the situation in the shielding problem for a nuclear-propelled airplane where a major fraction of the dose at the crew compartment is the air-scattered dose.

A shield designed to eliminate the penetrating radiation by scattering it into space may be termed a scattering shield. One way to achieve a scattering shield is by multiply-splitting the shield into a numberof segments between source and receiver. One

would expect that this would reduce the dose over a similar unsplit shield when the multiply scattered radiation constitutes most of the dose. Such multiply-split shields have been investigated in our study, principally in a disk geometry (source, receiver, and shield all coaxial disks or pillboxes of the same diameter) with dimensions typical of nuclear propelled space vehicles.

Another way to achieve a scattering shield is by proper placement of the shield, with respect to its location between source and receiver. Shield placement has been investigated in our study for disk geometry with dimensions typical of nuclear propelled space vehicles, for both split and unsplit shields.

The results of the present study indicate that the geometric attenuation factor due to splitting may be quite considerable for neutrons incident on non-hydrogenous shield material. For example, a dose decrease of a factor of 3 was obtained by splitting a carbon shield. The effect of shield splitting on neutrons incident on a hydrogenous shield was small. In some situations it increased the dose. The effect on the dose of splitting a gamma shield was also either small or adverse.

The results of the present study indicate that the geometric attenuation factor due to shield placement may be quite considerable for neutrons incident on a hydrogenous shield or for gammas incident on a Compton scatterer. It was found for example, that in either case when the shield is placed near the source the dose is a factor of 3 or 4 less than when the shield is near the detector.

These results are presented in detail in Section 4 of this report, in which the results of the Monte Carlo calculations are given. The tentative conclusions that have been deduced from these calculations and from analytical investigations are also given in Section 4. The basic qualitative ideas of the scattering shield are discussed in detail in Section 3. Simplified analytical methods are applied to obtain upper limits on the possible dose reduction by n-fold splitting of the shield. In Section 2, estimates are made for the required biological dose attenuation in manned nuclear rockets. The Monte Carlo codes and sampling methods are described in the Appendices.

It is important to emphasize the limited scope of the present study with regard to geometries and shielding materials. The study was confined almost completely to disk geometry. Only a few shield materials were considered and no inhomogenous shields were studied.

Section 2. Shielding Requirements for Nuclear Rocket Propulsion

In the absence of firm design data on nuclear rocket vehicle configurations we shall consider only schematic calculations of shielding requirements. We consider two basic vehicle types, both suitable for manned interplanetary missions. One is a hydrogen propelled vehicle operating at a thermal power of 1000 Mw for 30 minutes. The other is an ion propelled system that operates at 10 Mw thermal for one year. It is assumed that both vehicles start up from orbit, or in any case do not operate within the atmosphere, so that air scattering of neutrons and gammas is negligible.

The hydrogen-propelled vehicle was assumed to have a reactor payload separation distance of 180 feet and a diameter of 20 feet. (Some computations were also done for other diameters.) The reactor and payload faces were represented as discs of the same diameter as the vehicle, which was also taken as the shield diameter. Thus the shield was idealized as one or more cylindrical and coaxial discs of circular cross section.

The ion-propelled vehicle was assumed to have a reactor-payload separation of 50 feet with a diameter of 10 feet for some of the analysis, and a separation of 25 feet with a diameter of 5 feet for other calculations. The reactor and payload were taken as discs of the same diameter as the shield for most of the calculations. The calculations were therefore principally "one-dimensional" in the sense of Section 3. A few three dimensional calculations were performed, however, in which the reactor diameter was considerably

smaller than the shield.

The calculations are particularly concerned with two effect

1. The effect of splitting the shield into two or more segments, on the neutron and gamma transmitted dose at the payload.
2. The effect of changing the distance of the shield from the reactor and payload, on the neutron and gamma dose at the payload.

Such calculations have been investigated for both hydrogenous and non-hydrogenous shields.

We shall first estimate the required shield attenuation for the missions considered. With regard to neutrons we will assume that a total mission dose of 25 rem of neutrons is acceptable. Assuming an RBE of 10 and a flux-to-dose ratio for fast neutrons of 4×10^8 n/cm^2 per rep, this corresponds to a total fast nvt of 10^9 n/cm^2 at the manned crew compartment. If one neutron per second leaks from the reactor, the source intensity is given by

$$S = 3 \times 10^{16} P \text{ neutrons per second}$$

where P is the reactor power in megawatts. The integrated flux at the payload, in the absence of a shield, is then

$$\Phi t = \frac{St}{4\pi r^2}$$

where t is the effective time during which the source contributes to the dose, and r is the reactor to payload distance. The requi

shield attenuation factor, A, is then given by

$$A = \frac{10^9 \text{ n/cm}^2}{\phi t} .$$

In the hydrogen propelled system, if one ignores the attenuation by the propellant (a totally unjustified assumption) one obtains $A = 6 \times 10^{-6}$, corresponding to about twelve attenuation lengths. In the ion-propelled system one obtains for the 50 foot reactor-to-payload distance, $A = 3 \times 10^{-9}$, corresponding to about 19 attenuation lengths. It is clear that the ion propelled vehicle will require much more neutron shielding because of the much longer time at power.

The required attenuation factor in the hydrogen propelled rocket will be larger, i.e. less shielding will be required, than the figure given above, since the propellant will constitute the major part of the shield for most of the thrust period. This may be estimated as follows: We assume the initial propellant load to be a cylinder of hydrogen 150 feet long. Its length after t minutes is assumed to be

$$x(t) = x_o - vt$$

where x_o is the original length, and v is the number of linear feet which burn per minute. We have

$$v = \frac{x_o}{T}$$

where T is the total burning time. If all the hydrogen is used up

during the thrust period, the attenuation A_H that it provides is given by

$$A_H = \frac{1}{T}\int_0^T e^{-\frac{(x_o - vt)}{\lambda}}\, dt$$

$$= \frac{\lambda}{vT}\left(1 - e^{-x_o/\lambda}\right)$$

where λ is the neutron attenuation length in hydrogen, about 10 cm. Hence

$$A_H \cong \frac{\lambda}{x_o} \approx \frac{1}{450}.$$

The expression for A_H may also be interpreted as defining T_{eff}, an effective burning time for shielding purposes:

$$T_{eff} = \frac{\lambda}{x_o}\, T.$$

For the hydrogen propelled rocket this turns out to be about four seconds. Since a total attenuation of 6×10^{-6} is required, the actual shield (exclusive of the hydrogen propellant) must provide an attenuation, A_s given by

$$A_s = \frac{A}{A_H} \approx 3 \times 10^{-3}$$

corresponding to about six attenuation lengths.

We now consider the required attenuation of gamma rays for the two configurations. The allowable gamma dose over the mission will be taken as 25 rem, corresponding to an integrated energy flux of

$$\left(5.5 \times 10^5 \frac{\text{Mev}}{\text{cm}^2 \text{ sec r}}\right) \times \left(3600 \frac{\text{sec}}{\text{hr}}\right) \times (25 \text{ r}) \approx 5 \times 10^{10} \frac{\text{Mev}}{\text{cm}^2}.$$

We shall assume 4 3-Mev gammas are emitted per fission. The source intensity is given by

$$S_r = 1.2 \times 10^{17} P \qquad \text{Mev per second}$$

where P is the reactor power in megawatts. The integrated energy flux at the payload, in the absence of a shield is given by

$$\phi_\gamma t = \frac{S_\gamma t}{4 r^2}$$

The required shield attenuation factor, A_γ, is then given by

$$A_\gamma = \frac{5 \times 10^{10}}{\phi_\gamma t}$$

In the hydrogen propelled system, if one ignores the attenuation of the propellant one obtains $A_\gamma = 8.5 \times 10^{-5}$ corresponding to about 9.5 attenuation lengths. In the ion propelled system, one obtains for the 50 foot reactor-to-payload distance, $A_\gamma = 3.5 \times 10^{-8}$ corresponding to about 17 attenuation lengths.

When one considers the attenuation of the hydrogen propellant on gamma rays one obtains an attenuation factor

$$A_{H\gamma} = \frac{\lambda}{x_o} = 3 \times 10^{-2},$$

using $\lambda = 175$ cm for liquid hydrogen, leaving a required attenuation

factor for the shield material of

$$A_{s\gamma} = \frac{8.5 \times 10^{-5}}{3 \times 10^{-2}} = 2.8 \times 10^{-3}$$

corresponding to about 5.3 attenuation lengths.

These results are summarized in Table 1. From this table we conclude that the shields of interest range from 5 to 20 attenuation lengths in thickness for neutrons and gammas.

Some typical neutron removal cross section values and gamma attenuation coefficients are given in Table 1a for some high performance shielding materials. It is clear that in a linear (slab) geometry the neutron attenuation will be higher than the gamma attenuation for any low atomic weight material, and especially for hydrogenous materials. On the other hand, the gamma attenuation coefficients are higher for materials of high atomic weight, particularly at the higher energies. Hence a well designed shield will consist of both low and high atomic weight materials.

Table 1

Required No. of Attenuation Lengths

	Hydrogen-propelled		Ion-propelled
	Neglecting Propellant	Including Propellant	
Neutrons	11.3	5	19
Gammas	8.7	5.3	16.5

Table 1a

Typical Attenuation Coefficients for Neutrons and Gammas

	Neutrons (cm^2/gm)	3 Mev Gammas (cm^2/gm)	6 Mev Gammas (cm^2/gm)
LiH	.1525	.0353	.0300
CH_2	.1182	.0404	.0310
Be	.0713	.0313	.0212
Pb	.0099	.0413	.0445

Section 3. Qualitative Discussion of Shield Splitting & Placement

One can make analytical estimates of the effect of splitting and shield placement which are quite useful in setting upper bounds on the gains to be achieved by such shield designs. Furthermore, it is possible to evaluate many characteristics of the multiply-split scattering shield and of optimal shield configurations by qualitative arguments. In this section we give such analytic estimates and qualitative considerations.

The multiply-split scattering shield has been suggested as a means of eliminating buildup by scattering the deviated radiation into space. We have found that if the buildup contribution to the dose predominates over the unscattered radiation the dose can be reduced considerably by multiple splitting.

We have made simple analytic estimates of the shield weight savings achievable by splitting the shield. Assume a series of discs of equal radius between source and detector discs. The radiation leaving each disc has been assumed to have a cosine distribution. As an upper limit one can assume that all the neutrons or gammas which are scattered by a disc contribute to the buildup. Back reflection between discs will be neglected and the scattering cross sections will be assumed energy-independent. Then the fraction f(x) of radiation hitting a disc from the preceding disc is

$$f(x) = 1 + \frac{x^2}{2} - \sqrt{\left(1 + \frac{x^2}{2}\right)^2 - 1} \qquad (3.1)$$

where x is the distance between discs measured in units of the disc radius.

A more general form of this function can be given for discs of unequal radii, R_1 and R_2 at a separation distance L:

$$f(\alpha_1,\alpha_2) = \frac{1}{2}\left\{\left(1+\frac{\alpha_2^2}{\alpha_1^2}+\frac{1}{\alpha_1^2}\right) - \sqrt{\left(1+\frac{\alpha_2^2}{\alpha_1^2}+\frac{1}{\alpha_1^2}\right)^2 - 4\frac{\alpha_2^2}{\alpha_1^2}}\right\} \qquad (3.2)$$

where $\alpha_1 = R_1/L$, $\alpha_2 = R_2/L$.

These formulas were obtained by evaluating the following integral I over the areas of two discs of radii R_1 and R_2:

$$I = \int dx_2 dy_2 \cdot \frac{1}{\pi R_1^2} \int dx_1 dy_1 \frac{\cos\theta}{2\pi\left[L^2 + (x_2-x_1)^2 + (y_2-y_1)^2\right]} \qquad (3.3)$$

where the subscript 1 refers to the disc of radius R_1 and the subscript 2 to the disc of radius R_2. One disc is assumed to have uniform source intensity over its surface. The source radiation is assumed to have a cosine distribution with the normal to the discs. Here

$$\cos\theta = \frac{L}{\left[L^2 + (x_2-x_1)^2 + (y_2-y_1)^2\right]^{1/2}}$$

This integral was first evaluated by Walsh.[3] We have attempted to obtain similar analytic expressions for source radiation with other angular distributions. While it is easy to evaluate these integrals numerically no simple expressions analogous to (3.1) or (3.2) have been found.

We now return to expression (3.1) and apply it to a sequence of n discs equally spaced between source and receiver. The

assumptions of uniform source density, cosine angular distribution, and no back reflection, which are inherent in an iterated applicatio of (3.1) all tend to enhance the benefits of shield splitting. Most important of all, we shall assume that the penetrating radiatio consists predominantly of multiply scattered particles, which become the source for the next disc. This is equivalent to the assumption that the buildup is quite large. This assumption also enhances the effect of shield splitting in dose reduction. Hence this calculatio will give an upper limit to the geometric attenuation due to shield splitting. The geometric attenuation due to splitting the shield into n identical discs when the source-receiver distance is L is given by

$$\alpha(L,n) = \left[f\left(\frac{L}{n+1}\right)\right]^{n+1}$$

To compare the geometric attenuation of an n-fold split to attenuatic by an unsplit shield it is convenient to define a geometric improvement factor

$$I(L,n) = \frac{\alpha(L,1)}{\alpha(L,n)}$$

I is tabulated as a function of L and n in Table 2. Curves of I vs L for various n are given in Figure 1.

It can be seen that substantial improvement factors can be obtained for large L and n. A factor of 9.8 such as one gets for 3 discs with L = 12 corresponds to 2.3 mean free paths of shield thickness. This would save about 20% of the weight of a one-dimensio

shield with an attenuation of 10^5.

These analytic estimates presuppose that the multiply scattered radiation contributing to the buildup is so large as to be the preponderant contributor to the dose. Our Monte Carlo calculations have shown that this is very often not the case. We have estimated the buildup for neutrons in non-hydrogenous materials and found it to be quite large. In 15 mean free paths of a heavy nuclide with constant cross section, for example, one finds schematic figures of several thousand. In hydrogen, however, the neutron buildup is much less. For gamma rays the buildup is also much smaller.

TABLE 2

Shield Splitting Improvement Factor.
Analytical Formulas

L \ n	2	3	4	6	7	∞
6	1.7	2.2	2.5	2.7	3.0	3.4
8	2.3	3.5	3.7	4.9	6.8	9.2
10	3.0	6.0	9.1	14.9	19.3	30.4
12	4.0	9.8	17.9	36.4	45.2	113

One reason why the buildup in some cases is not as large as one might expect, even without splitting, lies in the relation between the finite size of the source and detector and the angular distribution of multiply scattered radiation. Scattered radiation is fairly evenly distributed in angle relative to the incident direction of the unscattered radiation, which we take as normal to the face of the shield. The conventional buildup factors which have been tabulated for gamma rays correspond to a detector inside the shield or in contact with the shield. When the detector is far from the shield, as it is apt to be in a space vehicle, only that part of the scattered radiation in the cone of angles that "see" the detector can contribute. Hence there is an important distinction to be made between the conventional buildup factor, which gives the ratio of multiply scattered to unscattered dose when the detector is in contact with the shield, and what one may call the effective buildup factor which gives the buildup ratio when the detector is far from the shield. When the shield disc is far from the detector much of the multiply scattered radiation will miss the detector anyway, regardless of whether the shield is split.

An estimate for the effective buildup factor in terms of the conventional buildup factor may be given for a single shield slab between source and detector. Let U be the probability that the radiation will penetrate the shield without scattering, and let S be the probability that scattered radiation will penetrate the shield surface. Then the effective buildup factor is given by

$$B_{eff} = \frac{\alpha_o U + \beta S}{\alpha_o U}$$

where α_o is the probability that a source neutron (or gamma) will hit the detector if no shield is present, and β is the probability that a scattered neutron (or gamma) that penetrates the shield will hit the detector. Now S may be related to the conventional buildup factor B:

$$S = \alpha_1 U (B-1)$$

where α_1 is the probability that a source neutron will hit the shield. Combining these equations one obtains

$$B_{eff} = 1 + \frac{\beta\alpha_1}{\alpha_o} (B-1)$$

The ratio $\frac{\beta\alpha_1}{\alpha_o}$ will normally be considerably less than unity when shield, source and detector are well separated. Hence the effective buildup factor will be less than the conventional one.

The directional character of the multiply scattered radiation is one factor in reducing the effective buildup. Another factor that is very important for gammas and for neutrons scattered in hydrogen is the energy-angle correlation in scattering.

When a gamma is scattered through a large angle it loses much of its energy. The Compton cross section at the new gamma energy is much larger, hence this gamma has a reduced probability of contributing. For a neutron scattered in hydrogen, too, large angle scattering results in large energy loss for the neutron, which then sees a higher cross section and has a reduced probability of contributing.

For a neutron scattered in a non-hydrogenous material this situation does not hold. Large-angle scatterings do not generally produce large energy changes and do not greatly reduce the chance of contributing. That is why one can find large buildup factors in non-hydrogenous materials.

Effect of Angular Distribution

The actual angular distribution of multiply-scattered neutrons is more forward peaked than a cosine distribution. This tends to increase the dose over the values indicated by the simple analytic estimates.

If one assumes that the radiation leaving a disc has a $\cos^n\theta$ distribution, the ratio of flux to current is given by

$$\frac{\phi}{J} = \frac{\int_0^{\pi/2} \cos^n\theta \sin\theta \, d\theta}{\int_0^{\pi/2} \cos^n\theta \cdot \cos\theta\sin\theta \, d\theta} = \frac{n+2}{n+1} \qquad (3.4)$$

Hence

$$n = \frac{1}{\frac{\phi}{J} - 1} - 1 \qquad (3.5)$$

An examination of flux-to-current ratios of some of our Monte Carlo results with the shield up against the detector gives values of n between 1.7 and 3.5. While the distribution is not of the form $\cos^n\theta$, the value of n is still a measure of the peaking of the angular distribution.

We see, then, that the flux is peaked more strongly than $\cos\theta$. Hence the actual gain due to splitting is less than the tabulated values of I(L,n) in Table 2.

Geometry Effect

An important aspect of optimal shield placement concerns the relative size of source and detector. If source and detector are discs of the same diameter we call the situation one-dimensional geometry or slab geometry. If the source is much smaller than the detector we call the situation three-dimensional geometry. In one-dimensional geometry adding one mean free path to the shield thickn adds shield mass proportional to the added thickness. In three-dimensional geometry the added mass required to increase the shield thickness by one mean free path is proportional to the square of the radius from the source to the shield edge. In three-dimensiona geometry one wants to place the denser materials on the inside of the shield at small radii.

Three-dimensional geometry penalizes the use of low density shielding materials since a given number of mean free paths must be placed at a greater radius. One-dimensional geometry does not discriminate between high and low-density material. The scattering shield can use low-density materials in one-dimensional geometry. Since splitting the shield is equivalent to lowering the average density, the three-dimensional situation attaches important shield weight penalties to splitting.

Another type of geometric consideration is also involved in the problem of optimal shield placement. Consider the optimal location of a single disc shield when source and receiver are the same size. It will depend on the source angular distribution and

the detector angular response. One can show by symmetry arguments that if these two functions are identical and if the shield attenuation is the same from either side, the optimal location is halfway between source and receiver. In general these two functions will not be identical nor will the shield attenuation be symmetric if it consists of several materials or if cross sections are strongly dependent on energy and if the scattered radiation is substantially degraded in energy. If one considers just the inverse square attenuations from source to shield and from shield to detector, the product of these two attenuations is minimized when the shield is centered. However, the optimal location still may be far from the midpoint.

The Monte Carlo calculations show, in fact, that the optimal location for a slab hydrogenous shield against neutrons is near the source, unless L is very large. This result is obtained for a cosine distribution of source neutrons. One can understand this by observing that in hydrogen the cross section increases sharply with decreasing energy and the unscattered neutrons are the most penetrating. If the shield is far from the source the neutrons are incident almost normally. If it is near the source many of the neutrons are incident at larger angles,and the average neutron suffers its first collision at a small distance into the shield. It then is degraded in energy and sees a larger cross

section, thus making the shield look thicker. This effect is most pronounced with isotropic neutrons and does not occur with a mono-directional beam normal to the source. The effect also disappears when the cross section is independent of energy. The net effect in one problem was to reduce the dose by 40% when the shield is moved from the mid-point to the source.

Even if the symmetry conditions hold one has a new optimal placement problem when splitting is admitted. One can show that moving material from the center increases the first-scattered dose while it decreases the multiply-scattered dose. Hence a new optimum must be found for a split configuration.

Section 4. Monte Carlo Calculation Results and Conclusions

The effects of shield splitting and placement on the transmitted dose have been quantitatively investigated by Monte Carlo procedures. The exploratory nature of the calculations imposed a number of restrictions on the program. The study was limited to shields composed of one material. Almost all the calculations were in one-dimensional geometry, in which no shield weight penalty is attached to use of low density materials. Only a few materials were studied. Nevertheless, the Monte Carlo results yielded a number of tentative conclusions, whose generality, however, is limited to the general type of situations studied.

These tentative conclusions will be presented briefly in Section 4.1. A description of the calculated geometries and materials is given in Section 4.2. The calculation results are presented and discussed in Section 4.3, where detailed evidence is given for the conclusions.

Section 4.1 Conclusions

The following tentative conclusions have been inferred from the Monte Carlo calculation results. Specific calculations to support these conclusions are cited in Section 4.3.

1. The neutron dose transmitted through a non-hydrogenous shield can be reduced appreciably by splitting the shield into two or more segments.

2. This dose reduction factor increases as L increases, where L is the source-to-detector separation distance (measured in units of source or detector radius), until L is sufficiently large that the unscattered flux predominates in the dose.
3. The neutron dose reduction due to splitting a non-hydrogenous shield increases with the thickness of the shield disc, up to some limiting thickness.
4. The neutron dose for L = 5 is minimized for a hydrogenous shield when the shield is near the source. The effect vanishes for large L, when a more centered shield gives the minimum dose.
5. The most disadvantageous location for hydrogenous shielding material is near the detector.
6. The gamma dose is minimized for small or moderate values of L when the shield is near the source and for larger values of L at more centered positions.
7. The most disadvantageous location for a gamma ray shield is near the detector.
8. Splitting a hydrogenous shield has no large effect on the neutron dose unless it moves shield material from near the source, in which case the neutron dose increases, at least for values of L in the neighborhood of 5. The effects of splitting seem to be (1) to decrease the dose somewhat for a fission source,

(2) to increase the dose somewhat for a 3 Mev source.

9. For a hydrogenous shield the effect of geometry on neutron dose is independent (within fairly wide limits) of both source energy and shield thickness.

10. Splitting has little effect on the gamma dose except when when the shield material is moved away from the detector.

It appears that splitting helps most for neutron attenuation in non-hydrogenous materials. In what shields will the design be determined by neutron attenuation through non-hydrogenous materials?

A. When non-hydrogenous material is used for shielding because it is already present for another purpose, e.g., a combination radiator and shield, or as a reserve cesium propellant in an ion propelled rocket.

B. When substantial amounts of gamma shielding material, which is non-hydrogenous, is incorporated in the shield.

C. In three-dimensional geometries where large neutron attenuations are desired, one will tend to use high density non-hydrogenous material instead of low density hydrogenous material.

D. When hydrogenous materials suffer from mechanical or containment difficulties.

Section 4.1 Description of Calculations

A set of Monte Carlo calculations was carried out for various axially symmetric configurations. The source was taken to be a disk, the detector a thin pillbox, and the shield one or more disks. Source, shield, and detector all had the same radius, in all except one pair of problems. In that pair, the shield was taken to be an approximation to a truncated cone.

The disk shield geometry was chosen as the simplest geometry that would demonstrate the effect of splitting and placement of shield material. Since realistic nuclear rocket configurations were not available, the geometry was simplified to source, shield, and detector. The source disk represents the side of a reactor and the detector represents a crew compartment. Materials were chosen for investigation to be typical of either shield, structure, or propellant. Again in view of the incompleteness of information about configurations, it was decided to investigate various relevant parameters in their effect on splitting and placement. These parameters included shield material, source spectrum, and geometry. The primary objective of the calculational program was then to determine the effect of geometry on dose.

In all the calculations, the overall shield thickness was small compared to the source-detector separation distance. The geometry can be specified by L, the ratio of source-detector separation to the radius; by the locations of the shield sections

along the axis, in fractions of L; and by ρt, the product of overall shield thickness and density. We use the symbol (0) to denote a configuration with the shield adjacent to the detector, $(\frac{1}{3}, \frac{2}{3})$ for a split shield with one segment 1/3 of the way from source to detector and the other segment 2/3 of the way, etc. For all the split shield configurations, all the shield segments were of equal thickness, except for two. The one denoted (0,1/2)* had 2/3 of the shield material in the piece next to the source and 1/3 midway between source and detector. The split tapered shield of Problem 25, which will be discussed below, did not have pieces of equal thickness, either.

A description of the problems done by Monte Carlo is given in Table 3 for gamma rays and in Table 4 for neutrons for those problems that either gave reliable results or else gave suggestive results of some intrinsic interest. We assign the greatest reliability to the results of problems numbered 51 and higher. Numerical results are given in Table 5 and 6.

Many of the problems described in Tables 3 and 4 were done for several cases simultaneously to save time by using a multicase option of the code. This feature is discussed in Appendix 1. One use of the multicase feature was to simulate shields of different thicknesses. Since the multicase feature requires that all the cases have the same geometry, a thinner shield is in fact simulated by reducing the density rather than the shield thickness. That is, only the product ρt, where ρ is the density and t the thickness, is relevant, rather than ρ and t separately. This w

be true as long as the shield thickness is small compared to both the diameter and the source-detector separation distance.

Where more than one case is listed for a problem, case 1 was always the case for which the sampling scheme was set up and usually (though not always) gave the best results.

Only the cesium problems, the carbon problems, and the water problems numbered from 51 up gave reliable results. The number of groups of histories run is listed for each problem. The group is the basic measure of the number of histories run, since there were always 100 histories per group. Problems listed in Table 6 with a suffix A, A_1, or B are reruns of the original problems and were done to obtain more groups. For such problems (53 and 53A, for instance), the results should be averaged. In the text, averages are used.

In some cases, two or more problems are shown in Table 4 for the same parameters. In these cases the Monte Carlo sampling scheme differs from one to the other. Only the results for the problem with the better sampling scheme are listed in Table 6.

In Tables 5 and 6, ϕ is the total flux and ϕ_n is the n-times-scattered contribution to the flux for $n \leq 4$. ϕ_5 includes all the 5-times and greater scattered radiation. The number in parentheses following each table entry is the fractional variance.

Problems run but not listed either duplicate more reliable computations which are listed or contain errors in the coding.

Hydrogenous neutron shields investigated were water, polyethylene, and lithium hydride. The polyethylene results were all unreliable and are not listed. In general, the lithium hydride results are less reliable than those for water, since water and not lithium hydride was always chosen as the base case (case 1) in the computation.

The most reliable results for nonhydrogenous materials were for carbon (graphite). The total cross section used was modified by smoothing some of the more violent fluctuations at higher energies which caused difficulty with the statistics of the Monte Carlo. For a fission source, the effect is probably very small, though reliable enough results for the unmodified cross section to prove it unambiguously could not be obtained. The problems with the modified cross sections are denoted by C-SP in Table 6.

It was desired to have some results for cesium, which would presumably be present in an ion-propelled rocket as propellant and which might be used for shielding. No cross sections have been measured for cesium. However, all the neighboring elements have smooth cross sections in the Mev region, which vary slowly in the same way for each one and whose magnitude changes from one nucleus to the next in a regular way. It is certain that cesium fits into this scheme. A constant cross section representation of cesium is denoted as Cs-SP in Table 6. Case 1 for the cesium disk problems (Problems 21-23) corresponds to a cross section of 7 barns

at normal cesium density of 1.88 and Case 2 to 4 barns at density 1.88. The cross section rises from about 4 barns to about 7 barns in the energy region of interest. For each case, the cross section was assumed constant and isotropic. The cesium shields considered were quite thin, since the primary purpose of the cesium is as a propellant rather than for shielding.

Problems 24 and 25 were for tapered geometries. The shield in Problem 24 was a set of successively larger cylinders which simulate a truncated cone. Problem 25 simulated a split tapered shield.

Several problems were done for iron, for an assumed constant and isotropic cross section. Iron was chosen as a typical structural material which might be used effectively for shielding if almost all of the attenuation were in fact by scattering out. Iron, unlike cesium, has a large number of resonances in the cross section and the constant cross section approximation is not a very good one. In addition, inelastic scattering was ignored because the code has no provision for it. The iron problems gave extreme difficulties in the sampling because of the larger number of collisions per history. No way could be found to sample adequately the histories containing many histories in a reasonable amount of machine time, for fairly thick shields ($\sim$2 feet). It seems that a less biased sampling scheme than the ones used will be best, but such a scheme will require many histories and long running times. The work and machine time required to evolve and

use such a scheme were not felt to be justified by the importance of the problem, which was rather unrealistic.

The gamma ray problems were all for materials of low atomic number, i.e., effectively Compton scatterers. In Problems 14 and 15 the shield material was polyethylene, both full and half density. In Problems 16-18, the shield material was hydrogen.

Since Monte Carlo is a statistical method, an ever-present concern is that the particular sampling scheme used may under-sample some important types of histories and not only give a bad answer (usually lower than the correct one), but give too low an estimate of the error. One can guard against this somewhat by running many histories, since in the limit of a very large number of histories the estimates will certainly be correct. One also wants to have an independent estimate for the answer to be really sure. In Problems 51 on, 1000 histories were run for each problem. The answers were quite stable over the last several hundred histories. With the sampling schemes used, it is felt that 1000 histories are sufficient for the hydrogenous and carbon shields. Since no independent estimate of the results existed, the sampling schemes were changed - that is, a different biasing was used - and some of the problems rerun. The idea was that the reruns would stress different types of histories than the original runs with the original sampling, and if the two runs agreed, the answer can be considered valid. Problems 66-69 are reruns with changed sampling.

Since the original sampling was chosen because it seemed satisfactory while the changes for Problems 66-69 were rather arbitrary, the original sampling gave less variance in the results. However, in all the problems, the results of both sampling schemes were in agreement. We can thus assert that for the problems done both ways, not only are the variances satisfactorily low, but the answers are substantially correct. Since a satisfactory sampling scheme for one problem will be satisfactory for problems which do not differ radically from that one, we can further assert that all the results for Problems 51-65 are substantially correct. Most of the earlier problems were run for only 500 histories and the results were not checked independently, so they are somewhat less reliable.

Table 3.

Shield Geometries and Materials - Gamma Rays

Problem No.	Shield Thickness(ft.)	L	Configuration	Case	Material	Density	Source Energy(Mev)
14	8.82	18	(0.82,1)	1	CH_2	0.92	1
				2		0.46	
				3		0.92	3
				4		0.46	
15	8.82	18	(1)	1	CH_2	0.92	1
				2		0.46	
				3		0.92	3
				4		0.46	
16	6.00	10	$(\frac{1}{2})$	1	H_2	0.521	3
17	6.00	10	$(\frac{1}{3}, \frac{2}{3})$	1	H_2	0.521	3
18	6.00	10	$(\frac{1}{5}, \frac{2}{5}, \frac{3}{5}, \frac{4}{5})$	1	H_2	0.521	3

TECHNICAL RESEARCH GROUP

Table 4

Shield Geometries and Materials-Neutrons

Problem No.	Shield Thickness(ft.)	L	Configuration	Case	Material	Density	Source Energy(Mev)
21	1.0	5	$(\frac{1}{4}, \frac{1}{2}, \frac{3}{4})$	1	Cs-SP	1.88	8
22	1.0	5	$(\frac{1}{2})$	2 1		1.074 1.88	8
23	1.0	5	$(\frac{1}{3}, \frac{2}{3})$	2 1	Cs-SP	1.074 1.88	8
24	Tapered; see discussion			2 1	Cs-SP	1.074 1.88	8
25	Tapered; see discussion			2 1	Cs-SP	1.074 1.88	8
29 35 36 39	2	10	$(\frac{1}{2})$	2	Fe-SP	1.074	8
30 37 40	2	10	$(\frac{1}{3}, \frac{2}{3})$		Fe-SP		8

Table 4 (continued)

Problem No.	Shield Thickness(ft.)	L	Configuration	Case	Material	Density	Source Energy(Mev)
31, 38, 41	2	10	$(\frac{1}{2}, 1)$		Fe-SP		8
32, 42	4	10	$(\frac{1}{2})$	1	H_2O	1.0	7
				2			3
				3			F
33, 43	4	10	$(\frac{1}{3}, \frac{2}{3})$		Same as (32,42)		
34	4	10	$(\frac{1}{5}, \frac{2}{5}, \frac{3}{5}, \frac{4}{5})$		Same as (32,42)		
47	2	10	$(\frac{1}{3}, \frac{2}{3})$	1	Fe-SP	7.8	8.0
48	2	10	$(\frac{1}{2}, 1)$	1	Fe-SP	7.8	8.0
49	2	10	$(\frac{1}{2}, 1)$	1	Fe-SP	7.8	8.0
50	2	10	$(\frac{1}{2})$	1	Fe-SP	7.8	8.0
51	2.5	5	(0)	1	H_2O	1.0	3
				2		0.5	
				3		1.0	F
				4		0.5	
				5	LiH	0.82	
				6	LiH	0.41	

TECHNICAL RESEARCH GROUP

Table 4 (continued)

Problem No.	Shield Thickness (ft.)	L	Configuration	Case	Material	Density	Source Energy (Mev)
52	2.5	5	(1)		Same as 51		
53	2.5	10	$(\frac{1}{2})$		"		
54	2.5	10	$(\frac{1}{3}, \frac{2}{3})$		"		
55, 68	2.5	5	$(\frac{1}{2})$		"		
56, 69	2.5	5	$(\frac{1}{3}, \frac{2}{3})$		"		
57, 66	2	5	$(\frac{1}{2})$	1	C-SP		F
				2			3
58, 67	2	5	$(\frac{1}{3}, \frac{2}{3})$	1	C-SP		F
				2			3
61	4	15	$(\frac{1}{2})$	1	C-SP	2.25	F
62	4	15	$(\frac{1}{3}, \frac{2}{3})$	1	C-SP	2.25	F
63	2.5	5	$(\frac{1}{2}, 1)$		Same as 51		
64	2.5	5	$(0, \frac{1}{2})^*$	1	H_2O	1.00	F
				2			3
65	4	15	$(\frac{1}{5}, \frac{2}{5}, \frac{3}{5}, \frac{4}{5})$	1	C-SP	2.25	F

Section 4.2 Results of Monte Carlo Calculations

A. Neutrons

Several series of problems were run for neutrons. The most complete set of problems for hydrogenous media are problems 51, 52, 55, 56, 63,64 for L=5. The results are given in detail in Table 6 and summarized in Table 7. If the dose for a shield next to the source is taken to be unity, the dose either for any of the split shields considered or for a single slab shield halfway between the source and the detector is about 1.4 or 1.5 and the dose if the shield is next to the detector is 4.2. These relative values refer to water. Similar relative values are given for lithium hydride.

Table 7. Comparative Doses for Hydrogen Shields 2.5 ft. Thick, L=5

Material	Water				Lithium Hydride	
Source Energy	3		F		F	
Density	1.0	0.5	1.0	0.5	0.82	0.41
Configuration						
(0)	1.0	1.0	1.0	1.0	1.0	1.0
$(0,\frac{1}{2})$*	1.3	-	1.4	-	-	-
$(\frac{1}{2})$	1.4	1.4	1.4	1.5	-	1.1
$(\frac{1}{3}, \frac{2}{3})$	1.9	1.7	1.3	1.4	-	0.9
$(\frac{1}{2}, 1)$	3.5	3.1	2.6	2.2	-	1.1
(1)	4.2	4.2	4.3	4.2	-	2.9

Table 7 indicates that there is a great choice of configurations for which the dose is not too much higher than its optimum value. The optimum is presumably achieved when all the shield is at the source, at least when L is as small as 5. The figures in Tables 6 and 7 show that it is extremely unlikely that any substantially different configuration will give appreciably better results or indeed will be nearly as good. The $(0, \frac{1}{2})^*$ configuration was investigated because it was surmised that it would give a lower dose than the (0) configuration. In fact, it turned out unmistakably higher. The split shield configurations show the large case-to-case variations. The $(\frac{1}{3}, \frac{2}{3})$ split is clearly better than the $(\frac{1}{2}, 1)$ split, though not than the $(0, \frac{1}{2})^*$ split. Since there was no appreciable saving from splitting, multiple splits were not investigated. Splitting seems to help somewhat with fission sourc and to hurt somewhat with 3 Mev sources, compared to a single centered disk.

The lithium hydride problems did not give as good statistics as the water problems. This occurred because the base case for th simultaneous calculations (see Appendix I) was chosen as a water shield. Thus the sampling was not too satisfactory for the LiH cases. In fact, the full density LiH case did not give any statistically useful results when the shield was adjacent to the detector, and the estimated errors were not small in any configura The half density LiH problem, corresponding to 1.25 ft. of ordinar LiH, shows little variation of dose with configuration, except tha

putting the entire shield next to the detector increases the dose by a factor of three over the other configurations considered. In both cases, while the computed fractional deviations ranged from 24-38 per cent, the results indicated some saving with splitting.

Problems 53 and 54, identical with problems 55 and 56 respectively [configurations $(\frac{1}{2})$ and $(\frac{1}{3}, \frac{2}{3})$] except with L = 10, gave quite similar results. Splitting had no effect, within statistical error, for the water problems, while for LiH it helped slightly.

A number of earlier problems were run for water and polyethylene for other shield thicknesses. While the results were not as reliable as those quoted, in no case did the results differ by more than 30-35 per cent or so between split and unsplit configurations.

The results for nonhydrogenous materials were more pronounced. For L = 5, splitting of a carbon shield reduces the dose by about 25 per cent. For L = 15, splitting once cuts the dose by about 60 per cent, i.e., by a factor of 2.5. The dose for a split into four pieces is about 1/3 of the dose for the unsplit shield. Since the 4-split the buildup factor is only 3, we infer that not too much will be gained by further splitting. The analytic formula of Section 3 indicates that the effect of splitting should increase with L, and that for large L multiple splitting can be effective. The analytic formula of Section 3 indicates that the effect of

splitting should increase with L, and that for large L multiple splitting can be effective. The Monte Carlo calculations bear this out, but show that the analytic formulas give a considerable overestimate for the effect of splitting, as one would predict from the rather strongly forward distribution of the scattered radiation.

The iron problems suggested that splitting helps for heavy elements. That is, lower doses were obtained for split than for unsplit configurations. However, all the statistics were so bad that one cannot regard these results as more than just suggestive.

The cesium calculations (Problems 21-23) showed little effect from splitting. Case 1 for Problem 22 gave a result which is probably somewhat high. The buildup was very small in these problems, so the results are not surprising.

The effect of splitting in a 3-dimensional geometry is illustrated by Problems 24 and 25. Here the ratio of separation distance to detector radius was 5 and that to source radius was 50 The total separation distance was 25 feet. The shield, for all practical purposes, was a truncated cone in Problem 24 that just shadowed the receiver from the source. It extended from 2 to 7.57 feet from the source. For Problem 25, the part of the cone betwee 5.8 and 7.57 feet from the source was moved outward and replaced by a truncated cone extending between 10 and 10.9 feet from the source. The total shield volumes are the same. The split shield gave a considerably higher dose because the total shield thickness was less and any beneficial

effect of splitting could not overcome the liability of a thinner shield. However, comparing the two problems, we see that for case 1, the unsplit shield gave a buildup factor of 7, while the split shield gave a factor of 4. For case 2 the numbers are 2.0 and 1.7 respectively. This splitting is helpful in cutting down the relative effect of multiply scattered radiation somewhat.

The gamma ray Problems 16-18 indicate that splitting is unimportant for Compton scatterers. Problem 16 is an unsplit centere shield, Problem 17 is a two-piece shield, and in Problem 18, the shield is split into four pieces. The flux for Problem 17 is somewhat higher than for the other two problems, but not by a large amount. Since neither the analytic treatment of Section 3 nor any general considerations lead one to expect that the result should be anything but monotonic in the number of splits, it is presumed that the larger result for Problem 17 is not real. No further problems of this sort were done for gamma rays, since any effect would be largest for Compton scatterers and less for heavy materials.

Problems 14 and 15 show the effect of moving some of the shielding away from the detector. Although the statistical errors in the calculations are not small, there is a clear substantial decrease in the dose on moving the material away. Only in Case 3 is this not clear, but in Problem 14 the error in this case is so large that the result is worthless.

One can sum up the results of the calculational program in the following conclusions:

1. The neutron dose transmitted through a non-hydrogenous shield can be reduced appreciably by splitting the shield into two or more segments.

   Problems 61, 62, and 65 show that a saving of at least a factor of 3 in the dose is possible.

2. This dose reduction factor increases as L increases until L is sufficiently large that the unscattered flux predominates in the dose.

   This is clear from the discussion of Section 3 and is borne out by a comparison of the results of Problems 57 and 58 with those of Problems 61 and 62.

3. The neutron dose reduction due to splitting a nonhydrogenous shield increases with the thickness of the shield disc, up to some limiting thickness.

   This follows from the fact that the dose reduction from splitting is limited by the amount of buildup, and buildup increases with shield thickness.

4. The neutron dose is minimized for a hydrogenous shield when the shield is near the source, for L = 5.

   This follows by comparison of the results of Problem 51 with those of Problems 52, 55, 56, and 63. When L becomes large, one can expect the optimum position to move away from the source toward the center, since the potential exists for a sizable

decrease in dose due to the inverse r^2 effect. For small values of L, the potential r^2 decrease cannot compensate for the effect discussed earlier that favors locating the shield near the source.

5. The most disadvantageous location for hydrogenous shielding material is near the detector. This follows from the results of Problems 51, 52, 55, 56, and 63.

6. The gamma dose is minimized when the shield is near the source, for small L. No calculations are available to support this conclusion. However, the same considerations that apply to neutrons in hydrogenous shields apply to gammas incident on a Compton scattering material. In fact, the stronger angle-energy correlation in Compton scattering makes the case even more emphatic.

7. The most disadvantageous location for a gamma ray shield is near the detector.

   This follows from the results of Problems 14 and 15 and the analogy with neutrons incident on a hydrogenous shield.

8. Splitting a hydrogenous shield has no large effect on the neutron dose unless it moves shield material from near the source, in which case the neutron dose increases for small or moderate values of L. This follows from the results of Problems 51, 52, 53, 54, 55, 56, 63 and 64.

   The effects of splitting seem to be (1) to decrease the dose somewhat for a fission source, (2) to increase the dose somewhat for a 3 Mev source.

This conclusion is more problematical than the others. It is suggested by the results of Problems 53, 54, 55, and 56.

9. For a hydrogenous shield, the effect of geometry on neutron dose is independent (within fairly wide limits) of both source energy and shield thickness.

   This is shown most clearly by Table 7.

10. Splitting has little effect on the gamma dose except when the shield material is moved away from the detector.

    This follows from the results of Problems 16-18.

Tables 5 and 6

In tables 5 and 6 results are given for the total flux, for ϕ_o, the unscattered flux, and for ϕ_n, the flux of particles experiencing n scatterings. The last column, ϕ_5, gives the flux of particles with 5 or more scatterings.

Table 5. Gamma Ray Fluxes for Various Shield Configurations

Material: Polyethylene
Source energy: 1 Mev
Total Shield Thickness: 8.82 feet
Shield Density: 0.92

Prob. No.	No. of Groups	Total ϕ	ϕ_o	ϕ_1	Flux by order of scattering ϕ_2	ϕ_3	ϕ_4	ϕ_5
14	4	9.0×10^{-10}(16)	5.3×10^{-11}(5)	1.4×10^{-10}(26)	1.5×10^{-10}(7)	1.9×10^{-10}(27)	1.2×10^{-10}(24)	2.5×10^{-10}(42)
15	4	1.4×10^{-9}(25)	4.9×10^{-11}(2)	1.0×10^{-10}(10)	1.7×10^{-10}(13)	2.9×10^{-10}(56)	1.2×10^{-10}(24)	6.5×10^{-10}(40)

Material: Polyethylene
Source energy: 1 Mev
Shield Thickness: 8.82 feet
Shield Density: 0.46

					Flux by order of scattering			
14	4	2.7×10^{-6}(6)	4.3×10^{-7}(5)	6.8×10^{-7}(21)	5.5×10^{-7}(7)	5.1×10^{-7}(33)	1.9×10^{-7}(18)	3.1×10^{-7}(22)
15	4	3.4×10^{-6}(14)	3.9×10^{-7}(2)	6.3×10^{-7}(4)	6.4×10^{-7}(8)	6.8×10^{-7}(40)	3.3×10^{-7}(22)	7.7×10^{-7}(37)

Material: Polyethylene
Source energy: 3 Mev
Shield Thickness: 8.82 feet
Shield Density: 0.92

					Flux by order of scattering			
14	4	9.1×10^{-7}(21)	1.5×10^{-7}(5)	2.3×10^{-7}(27)	1.9×10^{-7}(19)	1.5×10^{-7}(41)	8.2×10^{-8}(45)	2.9×10^{-8}(82)
15	4	7.8×10^{-7}(14)	1.4×10^{-7}(2)	1.7×10^{-7}(12)	1.8×10^{-7}(19)	1.7×10^{-7}(44)	4.6×10^{-8}(33)	6.8×10^{-8}(31)

Material: Polyethylene
Source energy: 3 Mev
Shield Thickness: 8.82 feet
Shield Density: 0.46 feet

					Flux by order of scattering			
14	4	6.6×10^{-5}(9)	2.3×10^{-5}(6)	2.1×10^{-5}(23)	1.2×10^{-5}(12)	6.7×10^{-6}(31)	1.9×10^{-6}(29)	1.3×10^{-6}(44)
15	4	6.2×10^{-5}(6)	2.1×10^{-5}(2)	1.8×10^{-5}(7)	1.2×10^{-5}(9)	7.1×10^{-6}(37)	2.0×10^{-6}(16)	2.2×10^{-6}(38)

Table 5 (continued)

Material: Hydrogen
Source energy: 3 Mev
Shield thickness: 6 feet
Shield density: 0.521

Prob. No.	No. of Groups	Total ϕ	Flux by order of scattering ϕ_o	ϕ_1	ϕ_2	ϕ_3	ϕ_4	ϕ_5
16	10	2.7×10^{-5}(12)	1.1×10^{-5}(11)	9.1×10^{-6}(19)	4.4×10^{-6}(29)	1.6×10^{-6}(30)	3.1×10^{-7}(41)	2.2×10^{-7}(29)
17	7	3.6×10^{-5}(15)	1.4×10^{-5}(10)	1.8×10^{-5}(25)	2.1×10^{-6}(26)	1.5×10^{-6}(42)	6.1×10^{-7}(40)	3.1×10^{-7}(30)
18	7	2.3×10^{-5}(13)	1.3×10^{-5}(13)	6.2×10^{-6}(34)	2.4×10^{-6}(27)	4.6×10^{-7}(56)	3.9×10^{-7}(46)	3.1×10^{-7}(38)

Table 6. Neutron Fluxes for Various Shield Configurations

Material: Water
Source energy: 3 Mev
Total shield thickness: 2.5 feet
Shield density: 1.0

Prob. No.	No. of Groups	Total ϕ	Flux by order of scattering ϕ_0	ϕ_1	ϕ_2	ϕ_3	ϕ_4	ϕ_5
51	5	4.3×10^{-8}(6)	5.7×10^{-9}(6)	7.2×10^{-9}(13)	1.0×10^{-8}(14)	7.3×10^{-9}(33)	4.1×10^{-9}(26)	8.9×10^{-9}(18)
51A	3	5.1×10^{-8}(13)	6.5×10^{-9}(11)	5.8×10^{-9}(7)	5.7×10^{-9}(18)	1.3×10^{-8}(40)	1.0×10^{-8}(37)	1.1×10^{-8}(19)
52	10	2.0×10^{-7}(5)	5.7×10^{-9}(4)	2.8×10^{-8}(21)	3.3×10^{-8}(12)	4.2×10^{-8}(11)	3.5×10^{-8}(16)	5.1×10^{-8}(20)
55	10	6.6×10^{-8}(7)	4.9×10^{-9}(8)	1.3×10^{-8}(8)	1.5×10^{-8}(16)	1.2×10^{-8}(21)	7.5×10^{-9}(18)	1.4×10^{-8}(21)
56	6	9.1×10^{-8}(14)	5.3×10^{-9}(8)	1.1×10^{-8}(20)	2.4×10^{-8}(30)	1.8×10^{-8}(31)	1.4×10^{-8}(13)	1.9×10^{-8}(32)
56B	6	9.4×10^{-8}(14)	5.0×10^{-9}(6)	1.1×10^{-8}(13)	2.1×10^{-8}(40)	9.7×10^{-9}(26)	1.9×10^{-8}(48)	2.8×10^{-8}(43)
63	10	1.7×10^{-7}(13)	5.8×10^{-9}(7)	1.9×10^{-8}(14)	3.6×10^{-8}(19)	3.9×10^{-8}(21)	2.3×10^{-8}(20)	4.4×10^{-8}(28)
64	10	6.4×10^{-8}(13)	5.7×10^{-9}(6)	9.6×10^{-9}(20)	1.8×10^{-8}(18)	1.5×10^{-8}(51)	8.8×10^{-9}(29)	7.2×10^{-9}(22)
53	5	7.2×10^{-9}(4)	2.2×10^{-9}(5)	1.8×10^{-9}(8)	9.7×10^{-10}(6)	9.2×10^{-10}(24)	5.8×10^{-10}(32)	7.4×10^{-10}(14)
53A	5	8.8×10^{-9}(14)	1.8×10^{-9}(4)	2.8×10^{-9}(35)	1.6×10^{-9}(15)	1.1×10^{-9}(30)	6.7×10^{-10}(32)	7.8×10^{-10}(29)
54	4	7.2×10^{-9}(11)	2.1×10^{-9}(12)	1.6×10^{-9}(18)	1.5×10^{-9}(30)	9.5×10^{-10}(17)	6.5×10^{-10}(41)	3.8×10^{-10}(10)
54A	6	9.1×10^{-9}(18)	1.9×10^{-9}(12)	2.4×10^{-9}(63)	1.2×10^{-9}(20)	1.5×10^{-9}(32)	9.3×10^{-10}(26)	1.2×10^{-9}(44)

Table 6(continued)

Material: Water
Source energy: 3 Mev
Total Shield Thickness: 2.5 feet
Shield Density: 0.5

Prob. No.	No. of Groups	Total ϕ	Flux by order of scattering ϕ_0	ϕ_1	ϕ_2	ϕ_3	ϕ_4	ϕ_5
51	5	4.5×10^{-5}(2)	1.4×10^{-5}(6)	1.0×10^{-5}(18)	1.0×10^{-5}(13)	5.9×10^{-6}(37)	1.7×10^{-6}(21)	3.2×10^{-6}(17)
52	10	1.9×10^{-4}(8)	1.4×10^{-5}(4)	4.3×10^{-5}(21)	4.0×10^{-5}(12)	3.3×10^{-5}(9)	2.2×10^{-5}(14)	3.6×10^{-5}(34)
55	10	6.4×10^{-5}(6)	1.2×10^{-5}(9)	1.9×10^{-5}(9)	1.6×10^{-5}(20)	8.2×10^{-6}(17)	3.4×10^{-6}(17)	5.1×10^{-6}(14)
56	6	7.5×10^{-5}(14)	1.3×10^{-5}(9)	1.8×10^{-5}(28)	1.9×10^{-5}(28)	1.1×10^{-5}(20)	7.5×10^{-6}(12)	6.2×10^{-6}(23)
63	10	1.4×10^{-4}(10)	1.5×10^{-5}(7)	2.7×10^{-5}(13)	3.9×10^{-5}(23)	3.1×10^{-5}(21)	9.8×10^{-6}(22)	1.7×10^{-5}(29)
53	5	9.0×10^{-6}(5)	5.1×10^{-6}(6)	2.2×10^{-6}(8)	6.7×10^{-7}(9)	4.3×10^{-7}(28)	2.8×10^{-7}(44)	3.0×10^{-7}(41)
53A	5	1.1×10^{-5}(16)	4.1×10^{-6}(4)	3.4×10^{-6}(34)	1.6×10^{-6}(31)	1.0×10^{-6}(45)	3.9×10^{-7}(29)	5.4×10^{-7}(47)
54	4	9.3×10^{-6}(14)	4.9×10^{-6}(13)	2.0×10^{-6}(18)	1.3×10^{-6}(41)	5.4×10^{-7}(22)	4.0×10^{-7}(35)	1.2×10^{-7}(26)

Table 6 (continued)

Material: Water
Source energy: Fission
Total Shield Thickness: 2.5 feet
Shield Density: 1.0

Flux by order of scattering

Prob. No.	No. of Groups	Total ϕ	ϕ_o	ϕ_1	ϕ_2	ϕ_3	ϕ_4	ϕ_5
51	5	4.3×10^{-7}(10)	7.5×10^{-8}(15)	8.7×10^{-8}(15)	1.1×10^{-7}(24)	7.5×10^{-8}(49)	2.8×10^{-8}(12)	5.5×10^{-8}(1
51A	3	4.4×10^{-7}(12)	8.0×10^{-8}(16)	8.2×10^{-8}(13)	8.5×10^{-8}(19)	6.3×10^{-8}(11)	5.2×10^{-8}(48)	8.3×10^{-8}(3
52	10	1.9×10^{-6}(13)	8.3×10^{-8}(6)	2.1×10^{-7}(12)	2.9×10^{-7}(14)	3.3×10^{-7}(20)	2.8×10^{-7}(41)	7.0×10^{-7}(2
55	10	6.0×10^{-7}(12)	7.1×10^{-8}(10)	1.2×10^{-7}(11)	1.6×10^{-7}(23)	6.5×10^{-8}(12)	5.0×10^{-8}(23)	1.3×10^{-7}(3
56	6	5.1×10^{-7}(11)	6.5×10^{-8}(9)	1.0×10^{-7}(20)	1.3×10^{-7}(26)	7.3×10^{-8}(24)	5.1×10^{-8}(19)	9.4×10^{-8}(12
56B	6	6.3×10^{-7}(14)	6.6×10^{-8}(17)	1.1×10^{-7}(13)	1.4×10^{-7}(30)	8.4×10^{-8}(18)	8.2×10^{-8}(26)	1.5×10^{-7}(25
63	10	1.2×10^{-6}(12)	9.3×10^{-8}(10)	2.1×10^{-7}(16)	2.5×10^{-7}(29)	2.3×10^{-7}(48)	1.0×10^{-7}(26)	2.7×10^{-7}(24
64	10	6.3×10^{-7}(6)	7.1×10^{-8}(6)	1.1×10^{-7}(13)	1.6×10^{-7}(26)	9.9×10^{-8}(37)	7.3×10^{-8}(23)	1.2×10^{-7}(34
53	5	6.2×10^{-8}(10)	2.9×10^{-8}(8)	1.7×10^{-8}(20)	5.4×10^{-9}(18)	4.6×10^{-9}(6)	2.7×10^{-9}(48)	4.6×10^{-9}(25
53A	5	8.8×10^{-8}(30)	2.7×10^{-8}(21)	3.9×10^{-8}(53)	7.5×10^{-9}(14)	6.2×10^{-9}(21)	3.8×10^{-9}(23)	5.0×10^{-9}(30
54	4	6.7×10^{-8}(20)	2.7×10^{-8}(36)	1.9×10^{-8}(35)	6.9×10^{-9}(12)	5.7×10^{-9}(33)	4.0×10^{-9}(55)	4.6×10^{-9}(54
54A	6	5.1×10^{-8}(15)	1.6×10^{-8}(10)	8.3×10^{-9}(17)	6.8×10^{-9}(31)	1.1×10^{-8}(28)	3.3×10^{-9}(31)	6.0×10^{-9}(67

Table 6 (continued)

erial: Water
rce energy: Fission
tal Shield Thickness: 2.5 feet
ield Density: 0.5

ob. o.	No. of Groups	Total ϕ	Flux by order of scattering ϕ_0	ϕ_1	ϕ_2	ϕ_3	ϕ_4	ϕ_5
1	5	3.8×10^{-5}(3)	1.4×10^{-5}(6)	8.2×10^{-6}(14)	8.0×10^{-6}(16)	3.2×10^{-6}(28)	1.4×10^{-6}(20)	3.1×10^{-6}(27)
2	10	1.6×10^{-4}(14)	1.6×10^{-5}(4)	4.1×10^{-5}(33)	4.0×10^{-5}(25)	2.3×10^{-5}(16)	2.0×10^{-5}(25)	1.8×10^{-5}(23)
5	10	5.7×10^{-5}(6)	1.3×10^{-5}(13)	1.6×10^{-5}(10)	1.3×10^{-5}(16)	7.4×10^{-6}(26)	3.1×10^{-6}(21)	3.5×10^{-6}(15)
6	6	5.2×10^{-5}(14)	1.4×10^{-5}(10)	1.4×10^{-5}(18)	1.0×10^{-5}(27)	5.2×10^{-6}(23)	5.1×10^{-6}(23)	2.8×10^{-6}(25)
3	10	1.1×10^{-4}(14)	1.6×10^{-5}(9)	2.4×10^{-5}(17)	2.5×10^{-5}(18)	1.9×10^{-5}(25)	1.8×10^{-5}(61)	8.8×10^{-6}(18)
3	5	8.6×10^{-6}(12)	5.0×10^{-6}(14)	2.1×10^{-6}(23)	5.0×10^{-7}(8)	6.1×10^{-7}(49)	1.2×10^{-7}(25)	2.6×10^{-7}(48)
3A	5	9.8×10^{-6}(14)	4.3×10^{-6}(12)	2.7×10^{-6}(30)	7.8×10^{-7}(18)	1.1×10^{-6}(51)	5.6×10^{-7}(65)	3.5×10^{-7}(24)
4	4	1.0×10^{-5}(20)	6.8×10^{-6}(26)	2.0×10^{-6}(29)	6.9×10^{-7}(37)	3.2×10^{-7}(9)	2.6×10^{-7}(74)	1.2×10^{-7}(41)

Table 6 (continued)

Material: Lithium Hydride
Source energy: Fission
Total Shield Thickness: 2.5 feet
Shield Density: 0.41

Prob. No.	No. of Groups	Total ϕ	Flux by order of scattering ϕ_o	ϕ_1	ϕ_2	ϕ_3	ϕ_4	ϕ_5
51	5	1.4×10^{-5}(31)	1.0×10^{-6}(4)	9.6×10^{-7}(14)	1.8×10^{-6}(18)	1.5×10^{-6}(31)	7.5×10^{-7}(14)	7.6×10^{-6}(56)
52	10	4.0×10^{-5}(23)	1.0×10^{-6}(3)	3.4×10^{-6}(18)	5.5×10^{-6}(31)	7.2×10^{-6}(21)	7.8×10^{-6}(44)	1.5×10^{-5}(27)
55	10	1.6×10^{-5}(25)	9.0×10^{-7}(8)	1.4×10^{-6}(10)	1.8×10^{-6}(14)	2.6×10^{-6}(34)	1.3×10^{-6}(25)	8.2×10^{-6}(46)
56	6	1.2×10^{-5}(24)	9.4×10^{-7}(9)	1.4×10^{-6}(22)	1.6×10^{-6}(23)	1.7×10^{-6}(25)	1.5×10^{-6}(31)	5.2×10^{-6}(38)
63	10	2.1×10^{-5}(21)	1.0×10^{-6}(7)	2.6×10^{-6}(16)	4.1×10^{-6}(34)	3.3×10^{-6}(25)	3.0×10^{-6}(38)	7.1×10^{-6}(45)
53	5	1.4×10^{-6}(20)	3.5×10^{-7}(9)	2.1×10^{-7}(15)	8.7×10^{-8}(9)	4.1×10^{-7}(76)	9.5×10^{-8}(22)	2.3×10^{-7}(50)
53A	5	1.2×10^{-6}(17)	3.2×10^{-7}(6)	2.3×10^{-7}(27)	2.1×10^{-7}(27)	8.3×10^{-8}(17)	9.2×10^{-8}(21)	2.4×10^{-7}(39)
54	4	1.1×10^{-6}(6)	3.6×10^{-7}(7)	2.0×10^{-7}(29)	1.8×10^{-7}(25)	7.0×10^{-8}(24)	1.6×10^{-7}(42)	1.2×10^{-7}(37)

Table 6 (continued)

Material: Lithium Hydride
Source energy: Fission
Total Shield Thickness: 2.5 feet
Shield Density: 0.82

Prob. No.	No. of Groups	Total ϕ	Flux by order of scattering ϕ_o	ϕ_1	ϕ_2	ϕ_3	ϕ_4	ϕ_5
51	5	7.1×10^{-8} (80)	4.0×10^{-10} (12)	8.0×10^{-10} (11)	1.8×10^{-9} (28)	6.8×10^{-10} (36)	6.5×10^{-10} (43)	6.6×10^{-8} (85)
52	10	3.4×10^{-8} (16)	4.5×10^{-10} (3)	1.9×10^{-9} (28)	2.9×10^{-9} (20)	8.8×10^{-9} (38)	5.0×10^{-9} (33)	1.5×10^{-8} (30)
55	10	2.7×10^{-8} (38)	4.1×10^{-10} (10)	1.2×10^{-9} (35)	1.3×10^{-9} (21)	1.9×10^{-9} (41)	1.1×10^{-9} (34)	2.1×10^{-8} (48)
56	6	1.1×10^{-8} (31)	4.1×10^{-10} (12)	8.1×10^{-10} (13)	2.7×10^{-9} (62)	1.2×10^{-9} (32)	1.1×10^{-9} (29)	4.8×10^{-9} (39)
63	10	2.0×10^{-8} (50)	4.4×10^{-10} (11)	1.0×10^{-9} (21)	1.7×10^{-9} (32)	1.3×10^{-9} (15)	2.4×10^{-9} (56)	1.3×10^{-8} (63)
53	5	1.4×10^{-9} (37)	1.2×10^{-10} (13)	1.7×10^{-10} (28)	1.2×10^{-10} (28)	4.9×10^{-10} (76)	5.1×10^{-11} (24)	4.9×10^{-10} (62)
53A	5	1.2×10^{-9} (26)	1.5×10^{-10} (19)	1.4×10^{-10} (14)	1.9×10^{-10} (36)	2.6×10^{-10} (61)	1.6×10^{-10} (46)	3.2×10^{-10} (32)
54	4	9.8×10^{-10} (31)	1.8×10^{-10} (21)	1.4×10^{-10} (34)	1.2×10^{-10} (33)	6.0×10^{-11} (27)	5.3×10^{-11} (45)	4.2×10^{-10} (62)

Table 6 (continued)

Material: Cesium (σ = 7 barns)
Source Energy: 8 Mev
Total Shield Thickness: 1 Foot
Shield Density: 1.88

Prob. No.	No. of Groups	Total ϕ	Flux by order of scattering ϕ_o	ϕ_1	ϕ_2	ϕ_3	ϕ_4	ϕ_5
21	7	8.7×10^{-3}(10)	5.8×10^{-3}(8)	1.3×10^{-3}(29)	5.3×10^{-4}(19)	3.7×10^{-4}(30)	4.1×10^{-4}(33)	3.9×10^{-4}(41)
22	6	1.2×10^{-2}(9)	5.8×10^{-3}(3)	1.2×10^{-3}(16)	9.5×10^{-4}(27)	7.4×10^{-4}(39)	2.9×10^{-4}(36)	2.8×10^{-3}(36)
23	6	8.5×10^{-3}(9)	5.5×10^{-3}(7)	1.2×10^{-3}(18)	6.7×10^{-4}(21)	3.0×10^{-4}(30)	3.0×10^{-4}(43)	5.4×10^{-4}(49)

Material: Cesium (σ = 4 barns)
Source Energy: 8 Mev
Total Shield Thickness: 1 Foot
Shield Density: 1.88

Prob. No.	No. of Groups	Total ϕ	Flux by order of scattering ϕ_o	ϕ_1	ϕ_2	ϕ_3	ϕ_4	ϕ_5
21	7	1.5×10^{-2}(9)	1.2×10^{-2}(8)	1.7×10^{-3}(29)	4.6×10^{-4}(21)	2.1×10^{-4}(30)	1.6×10^{-4}(34)	6.7×10^{-5}(38)
22	6	1.6×10^{-2}(4)	1.3×10^{-2}(3)	1.5×10^{-3}(16)	1.0×10^{-3}(36)	5.6×10^{-4}(47)	1.1×10^{-4}(34)	4.9×10^{-4}(36)
23	6	1.5×10^{-2}(7)	1.2×10^{-2}(7)	1.5×10^{-3}(18)	6.1×10^{-4}(24)	1.9×10^{-4}(40)	1.3×10^{-4}(48)	5.4×10^{-5}(35)

Material: Cesium(σ = 7 barns)
Source Energy: 8 Mev
Tapered Shield - See text for description
Shield Density: 1.88

Prob. No.	No. of Groups	Total ϕ	Flux by order of scattering ϕ_o	ϕ_1	ϕ_2	ϕ_3	ϕ_4	ϕ_5
24	7	1.0×10^{-7}(22)	1.4×10^{-8}(2)	8.7×10^{-9}(31)	6.1×10^{-9}(26)	7.1×10^{-9}(23)	6.5×10^{-9}(19)	6.0×10^{-8}(34)
25	6	2.8×10^{-7}(17)	7.1×10^{-8}(1)	2.7×10^{-8}(14)	2.3×10^{-8}(10)	2.3×10^{-8}(18)	4.9×10^{-8}(52)	8.3×10^{-8}(3[illegible])

Table 6 (continued)

Material: Cesium(σ = 4 barns)
Source Energy: 8 Mev
Tapered Shield - See text for description
Shield Density: 1.88

Prob. No.	No. of Groups	Total ϕ	Flux by order of scattering ϕ_o	ϕ_1	ϕ_2	ϕ_3	ϕ_4	ϕ_5
24	7	2.2×10^{-6}(7)	1.2×10^{-6}(2)	2.4×10^{-7}(8)	1.8×10^{-7}(18)	1.8×10^{-7}(29)	1.5×10^{-7}(32)	3.4×10^{-7}(35)
25	6	4.8×10^{-6}(6)	2.8×10^{-6}(2)	6.1×10^{-7}(15)	3.6×10^{-7}(11)	2.5×10^{-7}(18)	3.8×10^{-7}(47)	3.2×10^{-7}(34)

Table 6 (continued)

Material: Carbon (Graphite)
Source energy: Fission
Total Shield Thickness: 2 feet
Shield Density: 2.25

Prob. No.	No. of Groups	Total ϕ	Flux by order of scattering ϕ_o	ϕ_1	ϕ_2	ϕ_3	ϕ_4	ϕ_5
57A	6	2.0×10^{-5}(22)	5.2×10^{-7}(9)	1.0×10^{-6}(14)	1.1×10^{-6}(28)	1.0×10^{-6}(16)	2.2×10^{-6}(26)	1.4×10^{-5}(2
57A1	4	1.7×10^{-5}(16)	7.1×10^{-7}(6)	1.0×10^{-6}(19)	8.6×10^{-7}(22)	1.1×10^{-6}(36)	1.1×10^{-6}(28)	1.2×10^{-5}(1
58	10	1.5×10^{-5}(13)	4.8×10^{-7}(8)	8.5×10^{-7}(6)	1.0×10^{-6}(17)	1.5×10^{-6}(42)	9.0×10^{-7}(32)	1.1×10^{-5}(1

Material: Carbon (Graphite)
Source energy: Fission
Total Shield Thickness: 4 feet
Shield Density: 2.25

Prob. No.	No. of Groups	Total ϕ	Flux by order of scattering ϕ_o	ϕ_1	ϕ_2	ϕ_3	ϕ_4	ϕ_5
61	10	2.4×10^{-10}(23)	2.5×10^{-11}(21)	1.1×10^{-11}(23)	1.7×10^{-11}(31)	1.2×10^{-11}(28)	1.6×10^{-11}(21)	1.6×10^{-10}(29
62	6	1.1×10^{-10}(10)	1.6×10^{-11}(16)	7.8×10^{-12}(21)	1.1×10^{-11}(34)	1.6×10^{-11}(29)	9.4×10^{-12}(35)	5.2×10^{-11}(24
62A	4	7.5×10^{-11}(42)	2.7×10^{-11}(52)	6.9×10^{-12}(20)	8.6×10^{-12}(52)	7.9×10^{-12}(47)	3.6×10^{-12}(31)	2.1×10^{-11}(44
65	10	7.9×10^{-11}(21)	2.4×10^{-11}(34)	1.5×10^{-11}(15)	9.6×10^{-12}(24)	7.2×10^{-12}(21)	3.6×10^{-12}(22)	2.0×10^{-11}(36

Appendix 1. Description of Monte Carlo Codes

The two Monte Carlo codes developed to determine the effects of rocket shields compute respectively neutron and gamma transmission through a shield of complex design. Both current and flux at the detector are computed, along with their energy spectra, a partial breakdown of flux by order of scattering, and fractional standard deviations of all computed quantities. Since there is extensive overlap in the contents of the two codes, we will describe them together with separate discussion where necessary.

A. Geometry

The codes handle axially symmetric geometries. The source is a disk at one end of the configuration emitting radiation uniformly over its surface and the detector is a cylindrical cavity at the other.

The shield consists of a set of cylinders placed end to end. Each cylinder may be divided into a set of concentric pieces, which need not all be of the same material, and some or all of which may be void. The radial divisions which bound the pieces need not be the same in two different cylinders. The geometry is shown in Figure 1.

1. Gamma Rays

   Each piece is considered to be either a single element or a homogenous mixture of several elements.

2. Neutrons

   Each piece is considered to be one of three types: a homogeneous mixture of hydrogen and one other element, hydrogen alone, or one other element alone.

Figure 1. ILLUSTRATIVE SHIELD CONFIGURATION

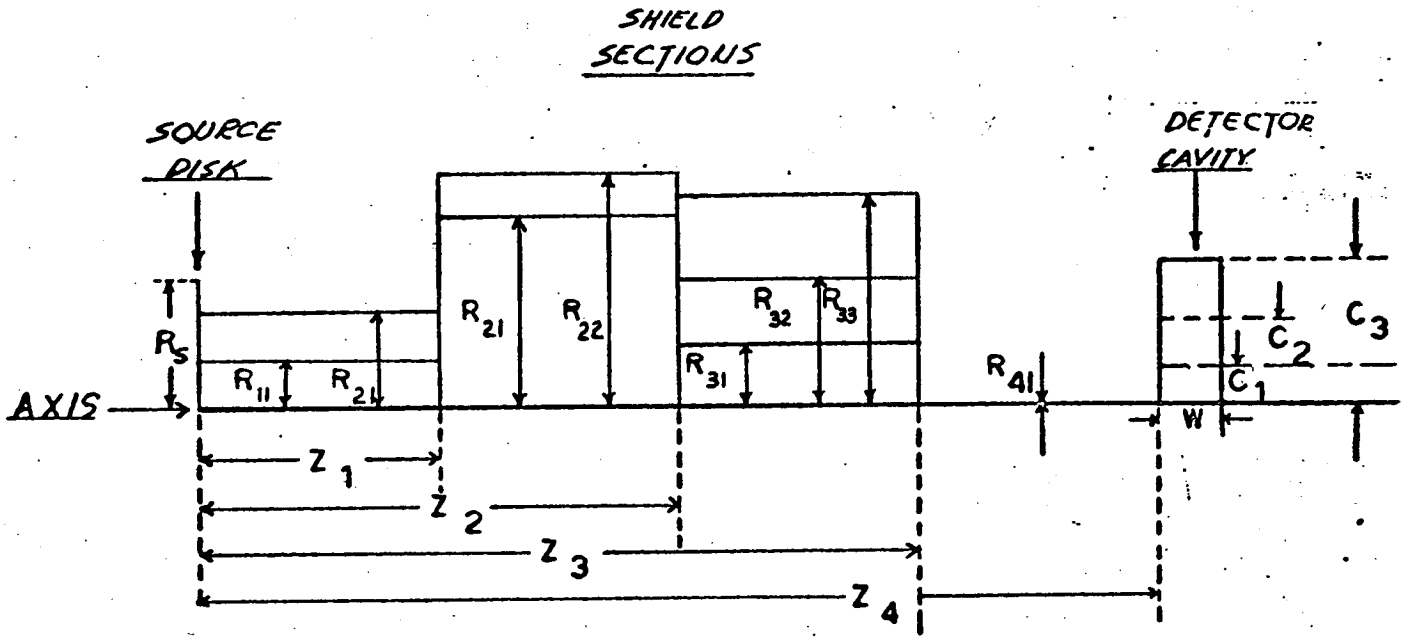

FIGURE ABOVE IS ROTATED COMPLETELY AROUND AXIS

B. Output

The detector is a cylindrical cavity which may be divided into concentric annular sections in order to obtain the radial dependence of flux and current. A flux is computed for each section as well as for the entire cavity, and is given by the total weighted track length per unit volume. The current is the total weighted number of particles entering the detector. The detector has generally, though not necessarily, been taken to be a very thin pillbox.

Current, flux in each detector section, and total flux are computed. We can get a breakdown by energy group as well as the totals. In addition, the total flux is accumulated by order of scatter, with flux after five or more collisions being lumped together.

For accumulation purposes (and also for random number generation), the histories in a given problem are divided into groups of a fixed number (usually one hundred). The resulting statistics are on a group to group basis. The two principal statistics calculated for any quantity are the mean T and the mean square S. Both are obtained from the group average A of the quantity. The mean T_n and mean square, S_n, after n groups, are computed as follows:

$$T_n = \frac{A + (n-1)T_{n-1}}{n}$$

$$S_n = \frac{A^2 + (n-1)\ S_{n-1}}{n}$$

The fractional deviation F is then determined, except for the first group, for each output quantity by the relation

$$F_n = \frac{1}{T_n} \quad \frac{S_n - T_n^2}{n-1} .$$

T_n and F_n are printed on-line after each group for total flux and current. F_1 is defined to be zero. T_n and F_n are printed off-line for all groups after the first, for all output quantities.

The units of output are as follows:

Gamma Rays

Flux - Mev/cm^2 sec

Current - Mev/sec (total current into detector).

Neutrons

Flux - neutrons/cm^2 sec

Current - neutrons/sec (total current into detector).

The division points for the energy groups are prescribed as input by giving an upper energy limit and a division width ΔE. The code can handle a maximum of ten energy divisions.

C. Source description

The source is assumed to be a disk of uniform intensity. The initial direction is given by one of two alternatives, a specific direction relative to the axis, i.e., a cone of radiation of fixed angle to the axial direction at each point on the source disk, or a given distribution of angles, restricted to integer (n) powers of cos θ, where $0 \leq n \leq 99$ and θ is the angle with the axis, $0 < \theta < \frac{\pi}{2}$. For both alternatives, the radiation is assumed to be uniformly distributed in azimuth.

1. Gamma Rays

The source is monoenergetic. For the computation of flux the source normalization is given as 1 Mev/cm^2 sec. For the current computation it is 1 Mev/sec from the entire source.

2. Neutrons

The source may be a monoenergetic source or else may have a fission neutron distribution. The normalization for the flux computation is 1 neutron/cm^2 sec. For the current computation it is 1 neutron/sec.

Note that with these normalizations the ratios of both flux and current to the appropriate source strengths are dimensionless quantities. For a thin detector the ratio of flux to current is just the average secant of the angle of the direction of the radiation entering the detector with the normal, multiplied by the ratio of source area to detector area.

D. Multicase Feature

Several problems may be run simultaneously by the code, if there are enough features in common. We then say we have a single problem with a number of cases. Specifically, variation among cases is allowed in the source energy and in the shield composition but not in geometry.

The variation in shield composition from one case to another is subject to some restrictions. In general a shield piece that is void for one case must be void for all cases. Furthermore, in the neutron code, any piece containing hydrogen in one case must contain hydrogen in all cases though the concentrations need not be the same and any other materials contained in the piece may be different. If a non-hydrogenous element is present in a piece in one case, one (not necessarily the same one) must be present in all cases.

The multicase feature is useful when the cases are not too dissimilar, so that the importance sampling used gives reasonable results for all the cases.

When several cases are computed simultaneously, the sampling scheme is chosen to be appropriate for the first one, as described below. The same histories are then used for all the remaining cases, with the characteristics of each case determining the weight factors that must be used. The particle trajectories are the same in all cases. However, if two cases have different source energies, the energies along any segment of the trajectory will be different.

E. Coordinates

1. Physical

The following variables describe the collision geometry:

a. Angle variables

δ = cosine of the angle between the ray and a line parallel to the axis of the system. (The axis is regarded as directed from the source to the detector).

ρ = cosine of the angle between the ray and an outward radius from the axis to the point of interest

Δ = cosine of the scattering angle

All azimuths are defined as an angle in a cone defined by δ around either the line through the point parallel to the axis, or around the direction before scattering at the reference point.

b. Spatial variables

z = distance from plane of source

R = perpendicular distance from the axis

2. Logical variables (internal to the code only)

The following variables are used by the code instead of ρ and R, for computational convenience.

η = $R\rho$ is used instead of ρ

S = R^2 is used instead of R

The set of quantities δ, ρ, z and R (or δ, η, z, and S) define the direction and position of a particle at any time. The first two will be termed the direction coordinates and the last two the position coordinates.

Figure 2 illustrates the collision geometry, showing the various angles.

Figure 2. TYPICAL GEOMETRY AT COLLISION

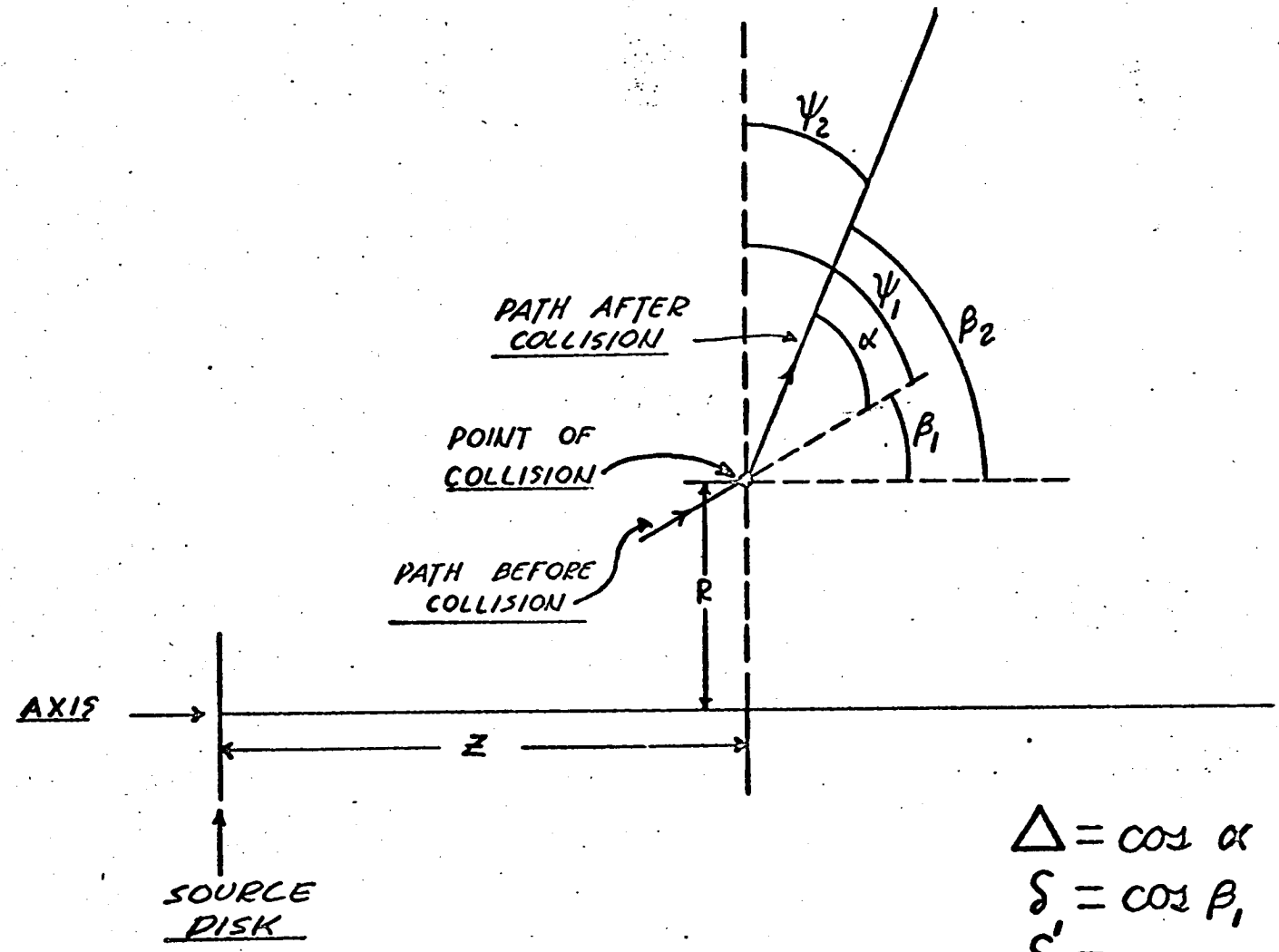

$\Delta = \cos \alpha$

$\delta = \cos \beta_1$

$\delta' = \cos \beta_2$

$\eta^* = R \cos \psi_1$

$\eta = R \cos \psi_2$

F. Initialization

1. Energy

a. Gamma Rays

For each case, the wavelength initially is that determined by the initial energy.

b. Neutrons

For each monoenergetic source case, the initial energy is the value as prescribed. For those cases where the initial energy forms a fission spectrum, the value for the given history is chosen* independently for each case.

2. Geometry

δ, the cosine of the angle made by the initial direction with the axis, is either chosen* from the given input distribution or else set equal to the initial value, as determined by input. For a distributed source in angle, δ is chosen initially from a distribution which cuts off at a lower limit of δ_{min}, the cosine of the largest angle with the axis for which a particle starting at some point on the source disk can see the shield or detector. The radial position and azimuth are then chosen* from uniform distributions, the radial position being uniform in S between S_{min} (the minimum value of S for which the shield or detector can be seen in the direction δ) and the edge of the source disk. The azimuth is chosen uniformly

*"Chosen" in this context means the variable is selected from a given probability distribution using the random variable procedure with the weight of the history accordingly adjusted.

between 0 and π or between $\pi/2$ and π, the latter if it is impossible to see the shield or detector (for the chosen S and δ) when the azimuth is between 0 and $\pi/2$.

3. Estimate of Unscattered Flux and Current

After the source conditions are set, the particle trajectory is calculated using the geometry calculation described below. Estimates of unscattered flux and current are made if the particle path intersects the detector. If the particle does not hit the shield at all, which in general can occur for certain source points and directions, the history is terminated. Otherwise, calculation proceeds to the selection of the point of collision.

C. Collision Loop

The basic collision loop goes as follows: Starting with a particle with a given direction and energy, either directly from the source or following a collision, the position of the next collision is chosen from an appropriate distribution. Absorption and escape are both forbidden, so that a subsequent collision always occurs somewhere in the shield, though not necessarily in the same piece. The direction and position coordinates of the particle at the collision point are then computed. A new energy and direction are chosen and the loop is repeated.

During the loop a statistical estimate is made. The

estimate procedure is different for neutrons than for gamma rays and is described separately.

A history is terminated either by Russian Roulette or by a low-energy cutoff when the energies for all the cases fall below a given cutoff energy. History termination is discussed below.

In general, the position and direction variables are chosen from distributions determined by the sampling scheme, discussed below. The particle weights must then be adjusted to compensate. The particular distribution from which any variable is chosen is determined in terms of a parameter which is a function of the state of the particle at the time.

The basic differences in the procedures in the collision loops in the neutron and gamma ray codes are that in the gamma ray code the statistical estimate is made after the new energy and direction are chosen, while in the neutron code it is made before. Further, the neutron code has a splitting provision lacking in the gamma ray code. In addition, the computation of direction after scattering proceeds differently in the two codes. There are also differences due to the different nature of the physical processes.

1. Distance Calculation

The mean free path distance x from the previous collision is chosen as some fraction of the distance D(in mean free paths) from the previous collision to the farthest edge of

the shield, so that escape is forbidden. The probability that the particle will not escape is automatically included as a weight factor, since the natural density function for the next collision position is e^{-x}, where x is the distance along the path in mean free paths. As a result the weight has an average factor of $\int_0^D e^{-x}\,dx = 1-e^{-D}$, which is the probability that the particle will not escape.

The distance Q in feet from the previous collision is then computed. Z^*, η^* and S^*, the values of Z, η, and S just before the collision, are determined in terms of the values Z_o, η_o and S_o after the previous collision by the formulas:

$$Z^* = Q\delta + Z_o$$

$$\eta^* = \eta_o + Q(1-\delta^2)$$

$$S^* = S_o + Q(\eta_o + \eta^*).$$

After the collision position is determined and before the choice of a new direction and energy, a test is made to see whether Russian Roulette (described below) is played. If Russian Roulette is not played, the collision loop continues by selection of a new direction and energy.

At a collision, absorption is forbidden; instead the weight is multiplied by the ratio of the proper differential scattering cross-section to the total cross-section. The average value of this quantity is simply the probability that absorption does not take place.

2. Collision Mechanics and Statistical Estimation

a. Gamma rays

Compton scattering, pair production, and photoelectric absorption are the only processes of interest and the latter two may be lumped as absorption. The cross-sections are described in Section J of this Appendix. The Klein-Nishina formula is used for the differential cross section.

For high energy gamma rays, Δ, the cosine of the scattering angle and ϕ, the azimuth about the direction before scattering, are chosen. The direction variables δ' and η' after collision are calculated from the following formulas in terms of η^* and δ, the values of the variables at the collision point preceding collision:

$$\delta' = \delta\Delta + \sqrt{(1-\delta^2)(1-\Delta^2)}\cos\phi$$

$$\eta' = \eta^*\Delta + \sqrt{\frac{1-\Delta^2}{1-\delta^2}}(\delta\eta^*\cos\phi-\alpha)$$

For low energy radiation, δ', the cosine of the angle with the axis, and the azimuth ϕ about the axis are chosen. Δ and η'/R, respectively the cosines of the scattering angle and the angle with the radius, are calculated according to the following formulas:

$$\Delta = \delta\delta' + \sqrt{(1-\delta^2)(1-\delta'^2)}\cos\phi$$

$$\eta' = \sqrt{\frac{1-\delta'^2}{1-\delta^2}}\,(\eta^* \cos\phi - \alpha)$$

In case $1-\delta^2=0$, Δ and ϕ are chosen and

$$\delta' = \delta\Delta$$

$$\eta' = \sqrt{S(1-\Delta^2)}\cos\phi$$

$$\alpha = \pm\sqrt{\left[S(1-\delta^2)-\eta^{*2}\right](1-\cos^2\phi)}$$

The sign of α is random, with both signs being equiprobable.

The energy variable used internally in the code is λ, the wavelength in Compton units:

$$\lambda = 0.511\ E^{-1},$$

when E is given in Mev. The increase in wavelength ($\Delta\lambda$) in a collision is given in terms of Δ by the relation

$$(\Delta\lambda) = 1 - \Delta$$

Thus once Δ is chosen the new wavelength is uniquely determined.

If for all cases the new wavelength is larger than the cutoff wavelength the history now terminates. If not, and the new direction is such that the particle would hit the detector if there were no further collisions, a statistical estimate is made for the surviving cases and then the history

proceeds. If a statistical estimate is not made and the history does not terminate, the history proceeds without an estimate back to the beginning of the collision loop.

For a statistical estimate, the distance D to the edge of the shield is computed. (D is always computed whether or not an estimate is made, since it is used for obtaining the next collision positi(.) The value of the estimate for the current is then

$$\frac{We^{-D}}{\lambda},$$

where W is the weight of the particle at the time the estimate is made, D is as before the mean free path distance along the ray to the farthest edge of the shield and λ is the wavelength. The flux estimate is obtained by multiplying the current estimate by the path length in the detector of the extended ray.

b. Neutrons

Hydrogen is treated differently than other elements because of the large average degradation in neutron energy in a collision with hydrogen. For hydrogen, the only process of any importance is elastic scattering in the center-of-mass system. For other elements elastic scattering and absorption are the only processes considered. Inelastic scattering is not taken into account. Anistropy in the differential elastic cross-section is allowed up to a P_1 term, that is, the differential cross section is assumed to be of the form

$$\frac{\sigma_{sc}}{4\pi}\,(1 + 3f_1\Delta_c),$$

where Δ_c is the cosine of the scattering angle in the center-of-mass system and σ_{sc} is the total elastic cross-section.

If both elements are present, a choice is made between the two as the collision element. If only one is present, the collision is obviously forced with that element.

If the collision is with hydrogen, the cosine Δ of the laboratory scattering angle and its associated azimuth ϕ about the direction before scattering are chosen at random. The resultant direction variables δ and η' and also the energy after collision for each case are calculated from the following formulas in terms of the variables at the collision point before collision:

$$\delta' = \delta\Delta + \sqrt{(1-\delta^2)(1-\Delta^2)}\,\cos\phi \qquad , \quad 1 - \delta^2 \neq 0$$

$$\eta' = \eta^*\Delta - \sqrt{\frac{1-\Delta^2}{1-\delta^2}}\,(\delta\eta^*\cos\phi - \alpha) \qquad , \quad 1 - \delta^2 \neq 0.$$

α has the same formula as in the gamma ray code.

If $1 - \delta^2 = 0$,

$$\delta' = \delta\Delta$$

$$\eta' = -\sqrt{S(1-\Delta^2)}\,\cos\phi.$$

The new energy is

$$E' = E\Delta^2.$$

The energy is then tested for each case. Those cases

for which it is below the cutoff energy are discontinued. When the energy for the last remaining case is below the cutoff the history is terminated.

If the collision is with an element other than hydrogen, the cosine of the angle with the axis, δ', and the azimuth ϕ_o about the axis are chosen. The cosine of the angle with the radius, η/R, the cosine of the scattering angle in the laboratory system Δ, the cosine of the center-of-mass scattering angle Δ_c, and the energy E' after collision are given by the following formulas:

$$\Delta = \delta\delta' + \sqrt{(1-\delta^2)(1-\delta'^2)}\ \cos\phi\ , \qquad 1-\delta^2 \neq 0$$

$$\eta' = \sqrt{\frac{1-\delta'^2}{1-\delta^2}}\ (\eta^*\cos\phi - \alpha)\ , \qquad 1-\delta^2 \neq 0$$

If $1-\delta^2 = 0$, $\Delta = \delta\delta'$

$$\eta = -\sqrt{S(1-\delta'^2)}\ \cos\phi,$$

Finally,
$$\Delta_c = \frac{\Delta^2-1 + \Delta\sqrt{A^2 + \Delta^2-1}}{A}$$

$$E' = E\left[1 + \frac{2A(\Delta_c-1)}{(1+A)^2}\right].$$

A is the atomic mass of the particular element, and therefore both Δ_c and E' depend on the case. As in the case of hydrogen, the energy is then tested for each case to determine whether it is below the cutoff.

We note that the procedure for hydrogen is analogous to that for high energy gamma radiation, while that for other elements is analogous to that for low energy gamma radiation. The reason is that for hydrogen and high energy gamma radiation large scattering angles imply large energy degradation and a much higher cross section for the next collision. The scattering angle then tends to be more important than the direction after scattering in determining the future of the particle. These considerations do not hold in the other situations, so the direction after scattering tends to be a more important determinant, since penetration is largest for particles moving in a forward direction.

The statistical estimate for neutrons is made after the collision point is determined and before the new direction and energy are determined according to the above formulas.

At the point of collision, the state (that is, position, direction, and energy) of the neutron is preserved in the memory. A ray is determined randomly from all those which intercept the detector by choosing the cosine δ' of the angle with the axis and an azimuth ϕ about the axis from appropriately truncated distributions. The truncation insures that the chosen ray intercepts the detector. The laboratory scattering angle and the angle with the radius are then calculated as follows:

For $S \neq 0$,

$$\eta = -\sqrt{S(1-\delta'^2)}\cos\phi$$

$$\Delta = \delta\delta' - \sqrt{\frac{1-\delta'^2}{S}}\,(\eta^*\cos\phi - \alpha) .$$

α is defined as before.

For $S = 0$,

$$\eta = 0$$

$$A = \delta\delta' + \sqrt{(1-\delta^2)\ (1-\delta'^2)}\ \cos\phi\ .$$

At this point, if hydrogen and another element are present, a choice is made (for estimate purposes) between them with the condition that if the cosine of the scattering angle is negative, the other element is automatically chosen. Given the element of collision, the weight of the neutron is adjusted according to the probability of actually being scattered through that scattering angle, and the energy after the collision calculated. Estimates are made for those cases in which the energies are not below the cutoff. The distance D to the far edge of the shield along the ray in mean free paths is computed. The value of the estimate for the current is We^{-D}, with the flux estimate being obtained by multiplying by the track length of the path extended through the cavity. After the estimate is made, the state of the neutron is restored, i.e., the position, direction, and energy stored in the memory are retrieved, and the new direction and energy are determined.

The statistical estimation is done in this way, so that an estimate can be obtained on virtually every collision. It was found previously, i.e., in an earlier version of the code, when the estimate was made following the determination of direction, that the process was quite inefficient. That is, relatively few

collisions gave estimates because most rays did not intersect the detector. With the new procedure, an estimate is obtained from almost every collision. An estimate is not obtained from every collision because the energy after collision computed in the estimate may be below the cutoff energy, in which case no estimate is made.

H. History Termination

1. Energy Cutoff for Degradation

In both codes the low energy cutoff can be given as optional input. If no value is specified in the input, the neutron code uses 0.33 Mev and the gamma ray code uses 0.0882515 Mev (K edge of lead).

2. Russian Roulette

Two test numbers are used in the Russian Roulette procedure. The first is a weight comparison quantity W_T, which has been set to 0.01 permanently in the code. The second quantity D_H is calculated in each history the first time a statistical estimate procedure is made in the history. For the neutron code this will be either from the source or after the first collision. For the gamma ray code it may be at any collision, since estimates are not forced. D_H is calculated as the sum of the distance to the collision point in mean free paths along the path travelled (zero if the first estimate is the source estimate) and the distance in mean free paths along the ray chosen at that estimate to the edge of the shield.

The procedure to establish whether or not Russian Roulette is played is in several stages (all this takes place immediately after the collision position is chosen). First the current weight is compared with W_T; if it is lower, Russian Roulette is played. If the weight is higher than W_T, a check is made to see whether D_H has been calculated for the history; if not, there is no further testing and Russian Roulette is not played. If there is a D_H for the history, $(D_H - \Sigma)$ is computed. Σ is the total mean free path distance along the particle path to the present collision position. If $(D_H - \Sigma)$ is positive, there is no further testing; if it is negative, the weight is multiplied by $\exp(D_H - \Sigma)$ and as a final test compared with W_T. If W_T is higher, Russian Roulette is played; otherwise the history proceeds.

The actual Russian Roulette procedure is quite simple. A random number is generated and compared with 0.1. If the random number is greater, the history is killed. If it is less than 0.1, the history continues multiplied by a weight factor of 10.

I. Splitting

Splitting was adopted for the neutron code when it was found that in some problems with nonhydrogenous shields some histories would go for 50 or 60 collisions and end up with very high weights. In these cases it was found that the weights did not rise much at any one collision; the high weights were cumulative effects. The splitting feature was added to the code in order to keep down the weights in such cases by in effect sampling such

histories more thoroughly. It was not found necessary for the gamma ray code and was not included there.

After the position of the collision is selected, a test is made to determine whether or not the history shall be split by dividing the estimate of the current at the next collision by a test quantity. If the quotient Q is greater than 8, splitting takes place, with the number of splits equal to $\frac{Q}{2}$, with up to a maximum of 256.

Splitting of splits may take place up to fortieth order.

The test quantity for the first group of histories is an unnormalized input quantity. For subsequent groups, the unnormalized average history contribution is used.

At the time of history termination, a test is made to see if the history was a split. If there are any remaining splits, the history returns to the point of the last unterminated split. When all the splits have been followed to death or cutoff, the history is terminated.

J. Cross Sections

1. Gamma Rays

The cross sections are stored in the code in the form of mass absorption coefficients and are the total cross sections in cm^2/gm for each material used. The argument table is wavelength (Compton units) ranging from .04 to 23.425*. Linear interpolation is used to obtain values of the cross section between tabulated values. The tabulated cross sections are based on Grodstein's tables.(3)

*See page 47 of Ref. 8

2. Neutrons

The total and scattering cross sections in barns/atom are stored in the code for each element used, while the first Legendre coefficient is in the usual normalized form. The argument table is energy in Mev ranging from 10.9 to 0.33. Linear interpolation is used to obtain cross section or coefficient values between tabulated values. The tabulated cross sections for H were those used by Aronson et. al.[4]; those for C were from the report of Kalos and Goldstein[7]; for O, Fe, and Si from Troubetskoy[9]; and for Li were obtained from Goldstein[2]. The tabulated first Legendre coefficients were modified so that the maximum value used was .3125, so that a realistic (positive) differential cross section would always be calculated. The scattering cross section used is the sum of the elastic and inelastic cross sections, although scattering itself was always considered to be elastic.

L. Random Number Generation

The fundamental generating procedure used to obtain random numbers first calculates random integers between 1 and $2^{35}-1$ by the multiplier-congruence procedure. The multiplier used is 5^{13} and the congruence is modulo 2^{35}. The random number is then scaled to be a fraction R between 0 and 1 by shifting the binary point 35 positions to the left. (IBM-704 numbers have 35 numerical bits.)

A generalized quota sampling procedure is used to modify the above generated number R for use in the random variable routine for the first 32 variables in each history. All other

times where random numbers are needed, the generated number is used directly.

The generalized quota sampling procedure is implemented (for each variable) by first considering the unit interval to be divided into N_G equal intervals $(\frac{K}{N_G}, \frac{K+1}{N_G})$, where N_G is the number of histories per group and K ranges between 0 and N_G-1. Call K the index of the subinterval. The basic procedure is then to force each random number for the variable to lie in a different subinterval for each history in the group. Let N be the number of unused subintervals; $M = N \times R + 1$; and K_M the index of the M^{th} unused subinterval. Then the random number R^* used is:

$$R^* = (N \times R - \lfloor N \times R \rfloor + K_M) / N_G$$

Thus

$$\frac{K_M}{N_G} \leq R^* < \frac{K_M+1}{N_G} .$$

Appendix 2. Sampling Procedure

In general, importance functions for problems of the sort handled by the codes are monotone in the particular independent variable being chosen. Therefore, as a simplification procedure, it was found desirable to chose each random variable from a one-parameter family of monotone distributions, in particular the truncated exponential. Thus we use a density function of form

$$f(u) = \frac{Be^{Bu}}{e^{B}-1},$$

where each random variable u is linearly scaled to be between 0 and 1 and B is a parameter defined by the state of the particle at the time u is chosen.

To determine the optimum choice of B, the minimax principle of game theory was adopted. This was done to insure maximum reliability in the results, a state not necessarily achieved by minimizing the theoretical standard deviation. That is, we want to choose B so as to minimize the weight for the worst possible choice of u.

Let g(u) be the importance function for the variable u, then the minimax principle is applied to the weight

$$h(u) = \frac{g(u)}{f(u)} = \frac{e^{B}-1}{B} e^{-Bu} g(u).$$

In general B can be determined by solving simultaneously

$$(1) \quad \frac{\partial h}{\partial B} = 0$$

$$(2) \quad \frac{\partial h}{\partial u} = 0.$$

(1) reduces to $$u = \frac{1}{1-e^{-B}} - \frac{1}{B}.$$

(2) reduces to $$B = \frac{d}{du} \ln g(u).$$

Note that if $g(u) = e^{Ku}$,

$$B = K.$$

(1) simplifies in certain limits, thus:

A. $B >> 0$, $u = 1 - \frac{1}{B}$

B. $B << 0$, $u = -\frac{1}{B}$

C. $|B| << 1$, $u = \frac{1}{2} + \frac{B}{12}$.

In many cases, examination of (2) allows (1) to be simplified to one of the above.

Let $\alpha(u) = \frac{d}{du} \ln g(u)$

Then the general problem can be expressed as solving for B:

$$B = \alpha\left(\frac{1}{1-e^{-B}} - \frac{1}{B}\right).$$

Derivation of Sampling Formulas

a) Gamma Rays

Most of the formulas for gamma ray transmission were based on formulas used in previous Monte Carlo gamma ray codes with changes being made on a trial and error basis. The minimax principle was used for the source direction and the low energy scattering procedure (where the variable selected was the cosine of the angle with the axis). The remaining source variables (which use the same formulas as the neutron code) were derived from essentially qualitative considerations.

b) Neutrons

The minimax principle was used to obtain most of the B formulas, exceptions being the source position and azimuth, and the azimuth for estimates or non-H scattering, which were based on qualitative considerations.

The formulas for the choice between hydrogen and non-hydrogen collision (H:N) were derived from qualitative considerations based on trial and error and previous coding experience.

Choice of Element

At the neutron collision point, for either the estimate or to continue the history it is necessary to make a choice between hydrogen and the other element as the collision nucleus. The general procedure (bypassed if either element is absent) is to calculate a quantity P_H (between 0 and 1) and to generate a random number. If the number is less than P_H, the collision is made with hydrogen and the weight divided by P_H. Otherwise the collision is made with the other element and the weight is divided by $1-P_H$.

$$P_H = \frac{K\sigma_H}{\sigma_t + (K-1)\sigma_H} ,$$

where at an estimate $K = 4\Delta^4$ if $\Delta > 0$

$K = 0$ if $\Delta \leq 0$,

at a collision to continue $K = 1/(8-4\Delta)$.

Sampling Parameters - Gamma Rays

Variable	u (Sampling Variable)	B (Sampling Parameter)
δ_o	$\frac{\delta_o - \delta_{MIN}}{1-\delta_{MIN}}$	$(3+n)(1-\delta_{MIN})$ (δ_o^n given source distribution)
S	$\frac{S-S_{MIN}}{S_{SO}-S_{MIN}}$	$-\frac{S_{SO}-S_{MIN}}{S_{DET.}}$
ϕ_o	(full range) $\frac{\phi_o}{\pi}$	Q
	(half range) $\frac{2\phi_o}{\pi} - 1$	Q/2
		where $Q = \frac{1}{2n}\left(\frac{1-\delta}{1-\delta_{MIN}}\right)\left(\frac{S_{SO}-S}{S_{SO}-S_{MIN}}\right)$
x	x/D	$D(\delta-1) - 1$
Δ	$(1+\Delta)/2$	$\delta U/(\lambda + 0.1)$ where $U = \min(2\delta(D-x), 8)$ if a statistical estimate was made at the last collision; $U = 8$ if no estimate at last collision
ϕ_Δ	$\frac{\phi_\Delta}{\pi}$	$(Z-Z_{DET})\sqrt{(1-\Delta^2)(1-\delta^2)}/R_{DET}$ $(1-\delta^2 \neq 0)$
		$S\sqrt{1-\delta^2}/S_{MAX}$ $(1-\delta^2 = 0)$

Sampling Parameters - Gamma Rays (continued)

Variable	u (Sampling Variable)	B (Sampling Parameter)
δ'	$(1+\delta')/2$	$U + \delta + 2(Z_{DET}-Z)/R_{DET}$ where $U = 6$ if $\delta \geq 0$ and no estimate at last collision; $U = 2\delta(D-x)$ if an estimate was made at the last collision
$\phi_{\delta'}$	$\phi_{\delta'}/\pi$	$-4\sqrt{(1-\delta^2)(1-\delta'^2)}$

Sampling Parameters - Neutrons

Variable	u (Sampling Variable)	B (Sampling Parameter)
E_o	$\frac{E_o - E_{MIN}}{E_{MAX} - E_{MIN}}$	0
δ_o	$\frac{\delta_o - \delta_{MIN}}{1 - \delta_{MIN}}$	$3.5 + 2\delta_{MIN} + n(1 - \delta_{MIN})$ (δ_o^n given source distribution)
S	$\frac{S - S_{MIN}}{S_{SO} - S_{MIN}}$	$-\frac{S_{SO} - S_{MIN}}{S_{DET}}$
ϕ_o	(full range) $\frac{\phi_o}{\pi}$	Q
	(half range) $\frac{2\phi_o}{\pi} - 1$	$\frac{Q}{2}$

where $Q = \frac{1}{2n} \left(\frac{1-\delta}{1-\delta_{MIN}}\right) \left(\frac{S_{SO} - S}{S_{SO} - S_{MIN}}\right)$

x	$\frac{x}{D}$	$D\left(\frac{1+R_\sigma}{2}\delta - 1\right)$
δ' (statistical estimate)	$\frac{\delta' - \delta_{LOW}}{\delta_{MAX} - \delta_{LOW}}$	$\left(\frac{\delta_{MAX} - \delta_{LOW}}{2}\right) \max(1, 2(D_1 - x\delta))$

where $D_1 = D\delta$ at first collision in history;
$D_1 = D_E \delta_E$ at subsequent collisions

Sampling Parameters - Neutrons (continued)

Variable	u (Sampling Variable)	B (Sampling Parameter)	
$\phi_{\delta'}$ (statistical estimate)	$\frac{\phi_{\delta'}}{\phi_{MAX}}$	$-\frac{\phi_{MAX}}{4}\sqrt{1-\delta'^2}$	$(S\neq 0)$
		$-\frac{\sqrt{(1-\delta^2)(1-\delta'^2)}}{4}$	$(S=0)$
δ' (non-H collision)	$\frac{\delta'+1}{2}$	$\min(2D_E\delta_E, \ln(0.92(\frac{3+R_\sigma}{1-R_\sigma})))$	$(R_\sigma\neq 0)$
		1	$(R_\sigma=0)$
$\phi_{\delta'}$ (non-H collision)	$\frac{\phi_{\delta'}}{\pi}$	$-\frac{\sqrt{(1-\delta^2)(1-\delta'^2)}}{4}$	
Δ (H collision)	Δ	5	$(\delta<0)$
		$(N+\sqrt{M^2+N})/2$,	$(\delta\geq 0)$,

where $M = D_E+3-Q$

$N = (QD_E+2Q-1)/8$,

where $Q = (\delta+P)D_E/(1-P)^2$

$P = D_E(\delta-1)$

Sampling Parameters - Neutrons (continued)

Variable	u (Sampling Variable)	B (Sampling Parameter)	
ϕ_Δ(H collision)	$\frac{\phi_\Delta}{\pi}$	$-\pi\sqrt{V/2}$	$(V \geq .5)$
		$-\pi V$	$(V < .5)$

where $V = D_E W/(1+D_E(1+W-\delta\Delta))$

$$W = \sqrt{(1-\delta^2)(1-\Delta^2)}$$

Definition of Symbols Appearing in Sampling Parameter Tables

Random Variables

Code	Symbol	Definition
n	E_o	source energy
n,γ	δ_o	source direction(cosine of angle with axis)
n,γ	S	square of distance from center(source)
n,γ	ϕ_o	source azimuth
n,γ	x	distance between collisions (mfp)
n,γ	δ'	cosine of angle with axis after collision
n,γ	$\phi_{\delta'}$	azimuth around axis
n,γ	Δ	cosine of scattering angle
n,γ	ϕ_Δ	azimuth around previous direction

These are the variables which are chosen randomly.

Definition of Symbols Appearing in Sampling Parameter Tables

Code	Symbol	Definition
n	E_{MIN}	minimum energy for fission
n	E_{MAX}	maximum energy for fission
n	δ_{LOW}	minimum cosine of angle with axis for which detector can be hit
n	δ_{MAX}	maximum of cosine of angle with axis for which detector can be hit
n	D_E, δ_E	D and δ from previous estimate
n	ϕ_{MAX}	maximum azimuth (given δ') for which detector can be hit
n	σ_H	hydrogen cross section (macroscopic)
n	σ_t	total cross section (macroscopic)
n	R_σ	σ_H/σ_t
γ	Z_{DET}	axial distance from source to detector
γ	R_{DET}	radius of detector
γ	Z	axial distance to collision point
γ	S_{MAX}	maximum radius squared of source, shield sections, and detector
γ	S	distance squared from axis to collision point
n,γ	δ_{MIN}	minimum cosine of source angle with axis for which shield or detector can be hit
n,γ	S_{SO}	source disk radius squared
n,γ	S_{MIN}	minimum possible radius squared for which (given δ_o) shield or detector can be hit
n,γ	S_{DET}	detector radius squared
n,γ	D	distance to edge of shield(mean free paths)
n,γ	δ	cosine of angle with axis before collision

Appendix 3. Generalized Quota Sampling

In Monte Carlo calculations, variance reduction techniques may be logically divided into two categories, those which reduce the expected variance of one sample, and those which reduce the variance of a sample of size N (faster than 1/N). Specifically if σ^2 is the expected variance of one sample, the expected variance σ_N^2 of a sample of size N is of the form:

$$\sigma_N^2 = f(N,\sigma^2)$$

In ordinary Monte Carlo, $f(N,\sigma^2) = \frac{\sigma^2}{N}$.

Quota sampling is a well known technique to reduce the variance faster than 1/N. Its chief drawback is that one has to make a "best" choice of a variable to be quota sampled or it will have very little effect on the results.

Using generalized quota sampling, i.e., quota sampling independently for all variables, an improvement is made in all cases.

Let $f(x_1,\ldots,x_n)$ be a bounded integrable function of n variables with $0 \le x_i \le 1$, all i.

Let $f_o = \int_o^1 \cdots \int_o^1 f(x_1,\ldots,x_n)\,dx_1,\ldots,dx_n$.

Let $\hat{f}(x_1,\ldots,x_n) = f(x_1,\ldots,x_n) - f_o$.

Let $f_i(x_i) = \int_o^1 \cdots \int_o^1 \hat{f}(x_1,\ldots,x_n)\,dx_1,\ldots,dx_{i-1}dx_{i+1},\ldots,dx_n$, all i.

Let $g(x_1,\ldots,x_n) = \hat{f}(x_1,\ldots,x_n) - \sum_i f_i(x_i)$.

Therefore $f(x_1,\ldots,x_n) = f_o + \sum_i f_i(x_i) + g(x_1,\ldots,x_n)$ where the decomposition is such that all terms are uncorrelated, allowing us to represent the variance of f as the sum of the variances of the individual terms. (This is shown in Lemma 3.)

Lemma 1: $\int_o^1 f_i(x_i)\,dx_i = 0$.

Proof: $\int_o^1 f_i(x_i)\,dx_i = \int_o^1 \cdots \int_o^1 \hat{f}(x_1,\ldots,x_n)\,dx_1,\ldots,dx_n$

$= \int_o^1 \cdots \int_o^1 f(x_1,\ldots,x_n)\,dx_1,\ldots,dx_n - f_o = f_o - f_o = 0.$

Lemma 2: $U = \int_0^1 \cdots \int_0^1 g(x_1,\ldots,x_n)\,dx_1,\ldots,dx_{i-1}dx_{i+1},\ldots,dx_n = 0$, all i.

Proof: $U = \int_0^1 \cdots \int_0^1 \hat{f}(x_1,\ldots,x_n)\,dx_1,\ldots,dx_{i-1}\,dx_{i+1},\ldots,dx_n -$

$$\sum_j \int_0^1 \cdots \int_0^1 f_j(x_j)\,dx_1,\ldots,dx_{i-1},dx_{i+1},\ldots,dx_n = f_i(x_i) - f_i(x_i) = 0,$$

(using Lemma 1 on $j \neq i$) .

Lemma 3: $\sigma_f^2 = \int_0^1 \cdots \int_0^1 \hat{f}^2(x_1,\ldots,x_n)\,dx_1,\ldots,dx_n = \sum_i \int_0^1 f_i^2(x_i)\,dx_i +$

$$\int_0^1 \cdots \int_0^1 g^2(x_1,\ldots,x_n)\,dx_1,\ldots,dx_n \equiv \Sigma\sigma_{f_i}^2 + \sigma_g^2 .$$

Proof: By Lemma 1, $\int_0^1 \cdots \int_0^1 f_i(x_i) f_j(x_j)\,dx_1,\ldots,dx_n = 0 \quad i \neq j.$

By Lemma 2, $\int_0^1 \cdots \int_0^1 f_i(x_i) g(x_1,\ldots,x_n)\,dx_1,\ldots,dx_n = 0$.
(omitting i^{th} integration)

Therefore, only square terms remain in expansion of $\hat{f}$.

Theorem: For each i, divide the unit interval into N intervals $(\frac{j-1}{N}, \frac{j}{N})$ and choose U_{ik} uniformly at random in an interval not previously chosen (independently for each i).

Let $\tilde{f} = \frac{1}{N}\sum_{k=1}^{N} f(U_{1k},\ldots,U_{nk})$.

Then $\sigma_{\tilde{f}}^2 \leq \frac{C}{N^2} + \frac{\sigma_g^2}{N}$ for sufficiently large N.

Note that for ordinary Monte Carlo $\sigma_N^2 = \frac{1}{N}(\Sigma\sigma_{f_i}^2 + \sigma_g^2)$

for a sample of size N, while for ordinary quota sampling

$\sigma_N^2 = \frac{k_i}{N^2} + \frac{1}{N}\left(\sum_{j\neq i} \sigma_{f_i} + \sigma_g^2\right)$ where i is the index of the quota sampled variable.

Proof: $\tilde{f} - f_o = \frac{1}{N} \sum_{k=1}^{N} \left(\sum_{i=1}^{n} f_i(U_{ik}) + g(U_{1k}, \ldots, U_{nk})\right)$

$$\overline{(\tilde{f}-f_o)^2} = \frac{1}{N^2}\left(\sum_{i=1}^{n} \overline{\left(\sum_{k=1}^{N} f_i(U_{ik})\right)^2} + \overline{\left(\sum_{k=1}^{N} g(U_{1k}, \ldots, U_{nk})\right)^2}\right).$$

All other terms are zero by the same argument as for Lemma 3. The bar here represents an ensemble average, that is, an average over all possible sample points.

To get an upper bound for the first term on the right, let

$$A_i = \sum_{k=1}^{N} f_i(U_{ik})$$

$$= \sum_{k=1}^{N} f_i(U_{ik}) - N\int_0^1 f_i(x_i)\,dx_i$$

$$= \sum_k \left\{ f_i(U_{ik}) - N\int_{\frac{k-1}{N}}^{\frac{k}{N}} f(x_i)\,dx_i \right\}$$

$$= \sum_k \left\{ f_i(U_{ik}) - f_i(\xi_k) \right\}, \quad \text{where } \frac{k-1}{N} \leq \xi_k < \frac{k}{N},$$

the last equality by the mean value theorem.

Rearrange the U_{ik} sequentially in k from k = 1 to N, and call the rearranged sequence U'_{ik}.

$$\left|A_i\right| \leq \sum_k \left| f_i(U_{ik}') - f_i(\xi_k) \right| \leq \max \left| f_i'(x) \right| = V_i.$$

Here

$$f_i'(x) = \frac{df_i}{dx} .$$

Then

$$\overline{\sum_{i=1}^{N} \left\{ \sum_{k=1}^{N} f_i(U_{ik}) \right\}^2} = \sum_{i=1}^{N} \overline{\left|A_i\right|^2} \leq \sum_{i=1}^{N} V_i^2 = C_1 ;$$

and

$$\overline{(\tilde{f}-f_o)^2} \leq \frac{C_1}{N^2} + \frac{1}{N^2} \overline{\left\{ \sum_{k=1}^{N} g(U_{1k},\ldots,U_{nk})^2 \right\}} .$$

The second term can be written

$$\overline{\left\{ \sum_{k=1}^{N} g(U_{1k},\ldots,U_{nk}) \right\}^2} = \sum_{k=1}^{N} \overline{g^2(U_{1k},\ldots,U_{nk})}$$

$$+ \sum_k \sum_{\ell \neq k} \overline{g(U_{1k},\ldots,U_{nk})\,(U_{1\ell},\ldots,U_{n\ell})}$$

$$= N\sigma_g^2 + N(N-1)Q.$$

To complete the proof, we must show that $Q \leq \frac{C_2}{N^2}$ for sufficiently large N. We have

$$Q = \frac{1}{N(N-1)} \sum_k \sum_{\ell \neq k} \overline{g(U_{ik},\ldots,U_{nk})\; g(U_{1\ell},\ldots,U_{n\ell})} .$$

In the ensemble averaging, U_{ik} is permitted to lie anywhere in the range (0,1). However, then $U_{i\ell}$ lies in the range J_k, which is the range (0,1) minus the subinterval L_k, of length $\frac{1}{N}$, containing U_{ik}. This must be true for each i. Thus

$$Q = \frac{1}{N(N-1)} \sum_k \sum_{\ell=k} \frac{\int_0^1 dx_n \cdots \int_0^1 dx_1 \int_{J_n} dy_n \cdots \int_{J_1} dy_1 \; g(x_1,\ldots,x_n)g(y_1,\ldots,y_n)}{\int_0^1 dx_n \cdots \int_0^1 dx_1 \int_{J_n} dy_n \cdots \int_{J_1} dy_1}$$

$$= \frac{1}{N(N-1)} \left(\frac{N}{N-1}\right)^n \sum_k \sum_{\ell \neq k} \int_0^1 dx_n \cdots \int_0^1 dx_1 \int_{J_n} dy_n \cdots \int_{J_1} dy_1 g(x_1,\ldots,x_n)g(y_1,\ldots,y_n)$$

Since the integral does not depend on k or ℓ,

$$Q = \left(\frac{N}{N-1}\right) \int_I^n dx_n \cdots \int_I dx_1 \; g(x_1,\ldots,x_n) \int_{J_n} dy_n \cdots \int_{J_1} dy_1 \; g(y_1,\ldots,y_n).$$

I is the unit interval, (0,1). $J_k = I - L_k$.

Lemma: $$\int_{J_n} dy_n \cdots \int_{J_1} dy_1 \; g(y_1,\ldots,y_n) \leq \frac{k}{N^2} + O(N^{-3}),$$

independent of $x_1,\ldots,x_n$, where $O(N^{-3})$ are terms of order $\frac{1}{N^3}$ and higher.

Proof: We define

$$(A_1,\ldots,A_n) = \int_{A_n} dy_n \cdots \int_{A_1} dy_1 \; g(y_1,\ldots,y_n).$$

Using the equivalence $I = J_k + L_k$, we break up $(J_n,\ldots,J_1)$ to separate integrals over subintervals containing different numbers of L_k. That is,

$$(J_1,\ldots,J_n) = (I-L_1,\ldots,I-L_n)$$

$$= (I,\ldots,I) - \sum_{k=1}^{n} (I,\ldots,L_k,\ldots,I)$$

$$+ \sum_{k=1}^{n-1} \sum_{\ell=k+1}^{n} (I,\ldots,L_k,\ldots,L_\ell,\ldots,I) + R.$$

R lumps together integrals over three or more of the L_k. The advantage of this decomposition is that terms containing p of the L-intervals are of order $1/N^p$. Now by lemma 2,

$$(I,\ldots,A_k,\ldots,I) = 0$$

for any A_k. Thus

$$(J_1,\ldots,J_n) = \sum_{k=1}^{n-1} \sum_{\ell=k+1}^{n} (I,\ldots,L_k,\ldots,L_\ell,\ldots,I) + O(N^{-3}).$$

Let $M = \max\left|g(y_1,\ldots,y_n)\right|$.

Then

$$\left|\int_{J_n} dy_n \cdots \int_{J_1} dy_1\, g(y_1,\ldots,y_n)\right| \le M \sum_{k=1}^{n-1} \sum_{\ell=k+1}^{n} \int_{J} dy_n \cdots \int_{L_\ell} dy_\ell \cdots \int_{L_k} dy_k \cdots \int_{I} dy_1$$

$$+ O(N^{-3}) = \frac{n(n-1)}{2} \frac{M}{N^2} + O(N^{-3}).$$

Thus the lemma is proved. We have then

$$Q \le \left(\frac{N}{N-1}\right)^n \left[\frac{n(n-1)}{2} \frac{M^2}{N^2} + O(N^{-3})\right] \le \frac{C_2}{N^2}$$

for sufficiently large N, as claimed. This is the final step in the proof. We have shown that

$$\sigma_{\tilde{f}}^2 \le \frac{\sigma_g^2}{N} + \frac{C}{N^2}.$$

Appendix 4. Operating Instructions for Monte Carlo Codes

Machine Requirements

The 704 required must have the following additions to the standard components:

a. 32K core memory

b. 5 tape units (only 4 normally used)

c. SHARE 2 board for on-line printer

d. Floating trap mode instructions (code will probably work without them)

Loading Procedure

1. First time - program run from cards

   Tapes

   4 - ready for program

   6 - output

   7 & 8 - temporary intermediate

   a. Place program followed by input in card reader

   b. Load program by pressing LOAD CARD

   c. Save tape 4 for later use (program tape)

   d. Input cards after program deck will be read in by program

2. Program run from program tape

   1 - program tape (physical tape prepared above)

   6 - output

   7 & 8 - temporary intermediate

   a. Place input, preceded by any corrections in card reader

   b. Load program by pressing LOAD TAPE

   c. Corrections (if any) and input will be read by program

3. Subsequent runs with preparation of new program tape

   Tapes

   1 - program tape

   4 - ready for new program tape

   6 - output

   7 & 8 - temporary intermediate

   a. Same as in 2 (difference in form of corrections).

   b. Same as in 2.

   c. Corrections will be read in by program and corrected program will be written on tape 4 (save this tape).

   d. Input will be read in by program.

Correction procedure

Once the program tape has been prepared, absolute octal corrections may be read in immediately preceding the input data. The general format for the corrections has the locations of the first correction in octal in columns 1-5 on the card, the number of corrections on the card in columns 6 and 7 in octal and the remaining, up to five, items are the corrections, 13 columns each in octal, loaded sequentially forward from the given initial location.

In addition, the count of the number of corrections is also used as an indicator to terminate the list of corrections (by setting it zero) and also to form a new program tape (by setting it less than zero). The usage of these cards is as follows:

a. no corrections

1 blank card ahead of each input set

b. corrections without new tape

corrections followed by 1 blank card ahead of first problem. 1 blank card ahead of each subsequent input set

c. corrections with new tape

corrections followed by card with negative count and then 1 blank card followed by input

1 blank card ahead of each subsequent input set.

Sense Switches

1 - down suppresses output tape writing (but not error printout)

2 - not used

3 - down ends problem after complete printout - inoperative if 1 is down

4 - down stops machine at end of problem and writes end of file on output tape

Press start with switch down to rewind output tape

Press start with switch up to start next problem

5 - down - on-line error print - if off-line error print takes place

6 - down - suppresses debugging printout if called for by input option.

Remarks on Input*

Format

Octal input is in octal integer notation.

Alphanumeric input consists of letters, numbers, and symbols which are ultimately to be printed in precisely the same form as they are put in.

Integer input consists of decimal integers.

Fixed point input is a decimal number of the form XX.XXX. The notation

Fixed (n)

under "Format" in the description of input preparation means that if the input number is put in without a decimal point, e.g., XXXXX, the code automatically puts the point n places to the left of the last digit. If the point is put in explicitly, the number is read with the point as indicated.

Shield Materials

Tables 8 and 9 are given for the code to identify shield components in Input Block 2. The components may be either elements or mixtures, for gamma rays, up to a maximum of 12.** The component code numbers range from 1 to 12. Since 10 components are given in the code (Table 8) only two new components, with code numbers 11 and 12, may be added without affecting data already there. If new components are listed with code numbers between 1 and 10, they replace the components already listed in the code with the corresponding code numbers. The same holds for neutrons except that

* See "Input Preparation", below.

**The word "mixture" or "material" in the subsequent text denotes a substance containing one or more of these 12 basic components.

Table 8.

Shield Component Table for Code for Input Block 2 (Gamma Rays)

Code Number	Component
1	H_2O
2	Pb
3	Be
4	CH_2
5	Al
6	W
7	Fe
8	U
9	Sn
10	H

Table 9.

Element Table for Code for Input Block 2 (Neutrons)

Code Number	Element
1	C
2	O
3	Al
4	Si
5	Fe

only 11 nonhydrogenous elements may be included. Hydrogen cross-sections are built into the code separately. Elements numbered 1 to 5 are listed in the code at present (Table 9).

Mixture Sets

The concept of a mixture set is used in describing the shield material in the input. Each shield piece consists of a given shield material in each case. In a multicase computation, the material need not be the same from case to case. The array of shield materials for a given piece of the shield as a function of the case is called a mixture set. Thus as an illustrative example, suppose there are four neutron shield substances, two mixture sets, and 3 cases. Suppose a portion of the input reads as follows:

Mixture card 1:	4,	4, 3, 6, 4
H density:		X_1, X_2, X_3, X_4
Non-H density:		Y_1, Y_2, Y_3, Y_4
Mixture set card 1:	2,3,1	
Mixture set card 2:	2,4,4	

The mixture card says that there are four mixtures. The non-hydrogenous substances are respectively elements numbers, 4, 3, 6, and 4 for the four mixtures, or shield materials. The element numbers designate the appropriate cross-section tables; the code is given in Table 9 below. Mixture 1 contains X_1 gm/cm^3 of hydrogen and Y_1 gm/cm^3 of element 4; mixture 2 contains X_2 gm/cm^3 of hydrogen and Y_2 gm/cm^3 of element 3, etc.

If the composition of a given shield piece is assigned as mixture set 1, the piece is assumed to consist of material (or mixture) 2 for case 1, of material 3 for case 2, and of material 1 for case 3. A shield section designated as consisting of mixture set 2 will be composed of mixture 2 in case 1 and of mixture 4 in the other two cases.

For gamma rays, the mixture cards are in a different format:

Mixture card 1 4(mixtures), 5(elements), 2,4,1,3,6

mixture 1: X_1, X_2, X_3, X_4, X_5

mixture 2: Y_1, Y_2, Y_3, Y_4, Y_5

mixture 3: Z_1, Z_2, Z_3, Z_4, Z_5

mixture 4: W_1, W_2, W_3, W_4, W_5

Here mixture 2 has element 2 at density Y_1, element 4 at density Y_2, etc.

Indicators

There are six indicators, $I_1, \ldots, I_6$, used in the input. In the normal case, they are all set equal to zero. If any of $I_1, \ldots, I_5$ is set unequal to zero a corresponding part of the input is skipped. (If I_2 is negative, there is extra input). This is desirable when that part of the input is already in the memory from the previous problem. If I_6 is unequal to zero, a detailed history trace is made.

Cross Sections

The energies at which the cross sections are tabulated are given in Tables 10 and 11.

Table 10

Wavelength and Energy Arguments for Cross Section Tables for Gamma Ray Code

Wavelength (Compton Units)	Energy (Mev)	Wavelength (Compton Units)	Energy (Mev)
.04	12.774	1.8	.284
.045	11.355	1.95	.262
.05	10.220	2.1	.243
.06	8.516	2.25	.227
.08	6.387	2.37	.216
.10	5.110	2.5	.204
.115	4.443	2.65	.193
.13	3.931	2.8	.182
.15	3.407	3.0	.170
.167	3.060	3.2	.160
.175	2.920	3.4	.150
.187	2.732	3.6	.142
.2	2.555	3.73	.137
.225	2.271	3.87	.132
.25	2.044	4.0	.128
.275	1.858	4.2	.122
.3	1.703	4.3929*	.116
.325	1.572	4.3929	.116
.35	1.460	4.6	.111
.4	1.277	4.8	.106
.45	1.136	5.0	.102
.5	1.022	5.2	.098
.55	.929	5.4	.095
.6	.852	5.6	.091
.65	.786	5.7905*	.088
.7	.730	5.7905	.088
.75	.681	6.38625	.080
.8	.639	7.3363*	.070
.9	.568	7.3363	.070
1.0	.511	8.515	.060
1.1	.465	10.218	.050
1.2	.426	12.7725	.040
1.35	.379	17.4667*	.029
1.5	.341	17.4667	.029
1.65	.310	23.425	.022

*K-edge discontinuities in U, Pb, W, and Sn respectively. Argument is repeated so that both values of the cross section at the discontinuities can be tabulated.

Table 11

Energy Arguments for Cross Section Tables for Neutron Code

Energy (Mev)	Energy (Mev)
10.9	1.90
10.4	1.81
9.89	1.72
9.41	1.63
8.95	1.55
8.51	1.48
8.10	1.41
7.70	1.34
7.33	1.27
6.97	1.21
6.63	1.15
6.30	1.096
6.00	1.042
5.70	.991
5.43	.943
5.16	.897
4.91	.853
4.67	.812
4.44	.772
4.23	.734
4.02	.699
3.82	.666
3.64	.632
3.46	.601
3.29	.572
3.13	.544
2.97	.518
2.83	.492
2.69	.468
2.56	.445
2.44	.424
2.32	.403
2.21	.383
2.10	.365
2.00	.347
	.330

Input Preparation

Card 1:	Format*	Spacing
a. Problem number and date	Alphanumeric	24
b. Descriptive material	Alphanumeric	48
Card 2:		
a. Initial random number	Octal	12
b. Number of histories per group($\leq$ 216)	Integer	6
c. Number of groups between output	Fixed point(0)	3
d. Collision limit	Integer	9
e. 6 indicators($I_1,\ldots,I_6$)	Integer	3 each(18)

Block 1

(Skip if I_1 not zero)

Card 1:		
a. Number of mixture sets($\leq$ 10)	Integer	3
b. Number of cases($\leq$ 15)	Integer	3
c. For each case, source energy, maximum energy for spectrum, width of spectral division.[a]	Fixed point(0)	5 each (15 per case)

Subsequent cards (if more than 4 cases)

a. For each case, source energy, maximum energy for spectrum, width of spectral division.[b]

*See notes for Input, above.

a. First four cases.
b. Four cases per card; start at beginning of each card.

Block 2 (Gamma Rays)

Test I_2 (skip entirely if positive)

If I_2 negative, start here; if I_2 zero, skip:

Card 1

a. Number of new components (total number of components $\leq$ 12)	Integer	3
b. Space		3
c. Code number for each new component	Integer	3 each

For each new component, there is a sub-block of cards:

Card 1

a. Symbol	Alphanumeric	6
b. First 11 entries of total cross section	Fixed(3)	6 ea.(66)

Cards 2-6

All remaining cross section entries.[a]	Fixed(3)	6 ea.(72 per card)

If I_2 zero, start here; continue here also if I_2 is negative:

Card 1

a. Number of mixtures ($\leq$ 12)	Integer	5
b. Number of components used in problem ($\leq$ 6)	Integer	5
c. Component code numbers	Integer	5 each

Subsequent cards (one for each mixture)

Density (gm/cm^3) of each component in mixture[b,c]	Fixed(5)	10 each

[a] There are 70 entries in each cross section table, plus the electron density as entry 71.

[b] Density = 0 for components used in problem but not included in mixture.

[c] Densities are given for various components in the same order as the component code numbers appear on Card 1.

Block 2 (Neutrons)

Test I_2 (skip if positive)

If I_2 negative, start here; if I_2 zero skip:

Card 1

a. Number of new elements (total number of nonhydrogenous elements ≤ 11)	Integer	3
b. Space		3
c. Code number for each new element	Integer	3 each

For each new element there are 19 cards:[a]

Card 1

a. symbol	Alphanumeric	6
b. atomic weight	Fixed(2)	6

6 cards of total cross sections

12 per card (11 on last card)[b]	Fixed(2)	6 each

6 cards of scattering cross sections

12 per card (11 on last card)[b]

6 cards of coefficients of first Legendre polynomial

12 per card (11 on last card)[b]

If I_2 zero start here; continue here also if I_2 is negative:

Card 1

a. Number of mixtures (materials) used in problem (≤ 6)	Integer	5
b. Space		5
c. Code numbers of non-H elements	Integer	10 each

[a] The elements are arranged as in the code number list.

[b] There are 71 entries in the cross section list.

Card 2		
a. Space		10
b. H densities for each mixture[a]	Fixed(5)	10 each
Card 3		
a. Space		10
b. Non-H densities for each mixture[a]	Fixed(5)	10 each

Code numbers, H densities, non-H densities in correspondence

Block 3

Test I_3 (if not zero, skip)[b]

One card for each mixture set:		
For each case, the mixture number giving the composition of the given mixture set[b]	Integer	3 each

Block 4

Test I_4 (if not zero skip)

Card 1		
a. Number of axial divisions of shield ($\leq$ 16)	Integer	3
b. Number of radial divisions of cavity ($\leq$ 8)	Integer	3
c. Width of cavity (feet)	Fixed(2)	7
d. Radial divisions(feet) of cavity from inner to outer	Fixed(2)	7

[a] The non-H element code numbers, hydrogen densities, and non-H densities must all be given in the same order.

[b] If I_3 is negative or if there is only one case, each mixture set is assigned the corresponding mixture number by the code; that is, mixture set 1 consists of shield material (mixture) 1, etc.

Card 1

a. Upper end of axial division of shield section	Fixed(2)	9
b. Number of radial divisions ($\geq 1, \leq 8$)	Integer	3
Subblock, repeated at most 5 times:		
c. Outer radius of division (feet)[a]	Fixed(2)	9
d. Mixture set number of division (0 indicates vacuum)	Integer	3

Card 2, if needed.[b]

a. Space		12
Subblock, repeated at most 3 times:		
b. Outer radius of division (feet)[a]	Fixed(2)	9
c. Mixture set number of division	Integer	3

Block 5

Test I_5 (if not zero skip)

1 card

a. Power of cos θ_0 for distributed source ($\geq 0, \leq 99$)	Integer	2
b. Initial direction cosine (0 means distributed)	Fixed(4)	7
c. Radius of source disk (feet)	Fixed(2)	9
d. Minimum energy for calculation (Mev)[c]	Fixed(7)	9

---

[a] Radial divisions must be in order of increasing radius.

[b] A second card is need if there are 5 or more radial divisions. If there are just 5 divisions, the second card is blank.

[c] Zero means to use the coded value.

Debugging and Error Tracing Procedure

By setting I_6 (see input) not equal to zero, a collision-by-collision trace will be made. Further, sense switch 6 may be used to control the amount of trace.

In addition, a similar printout (on tape) is made each time certain errors occur within the collision loop. Also, using sense switch 5, the same printout may be obtained on-line.

The possible printout conditions and their indicators are given in Table 12. The contents of each printout and their titles are given in Table 13.

Table 12

Error Indicator Names

NONE	Indicator = 0	input option (I_6= 0)
NONE	Indicator = 1	quotient underflow
-SINSQ		cosine of angle with axis greater than 1 in magnitude
DCT-SE		divide check detected while calculating distance to edge
-I,SE		negative axial position indicator
ESCAPE		collision point calculated to be outside of shield
I BIG		axial position indicator above maximum possible
PATHD		more than 40 sections in path along ray
-R.V.		random variable less than zero or greater than one
R.N.		bug in random number generator (now impossible)
SQRT		negative argument for square root
LOG		negative or zero argument for log
EXP		argument greater than or equal to 64 for exponential
DCT-PO		divide check detected while finding collision position

Histories are terminated at all true errors (i.e. if title is anything but "NONE")

Table 13

Error Printout Data

(Title)	indicator
GP.	group number
HIS.	history number within group
COL.	collision number within history
TOTCOL.	total number of collisions
ST.EST.	total number of estimates
Z-I.	present axial division number
R-I.	present radial division number
CURRENT	last calculated current estimate
MFP-EDGE	distance to edge in mean free paths
MFP-TOT	total distance travelled in mean free paths*
WT-CASE	weight of case one particle*
FIX-WT	universal weight of particle*
ENERGY(Neutron)	neutron energy
WAVE(Gamma)	gamma ray wavelength
SCAT.	cosine of scattering angle
AZIM.	azimuthal angle at scattering
COS.Z	cosine of angle with axis
COS.R/BE.	cosine of angle with radius before scattering
AF.	cosine of angle with radius after scattering

*At every ten collisions in each history the fixed weight is set to 1. The weight for each case is set between 1/2 and 1 (the fractional part of the product with the fixed weight) and the total mean free path for each case adjusted by the proper multiple of $\ell n 2$.

Table 13 (continued)

R.DIST.	distance from axis of collision point (feet)
Z.DIST.	distance along axis of collision point (feet)
BET.COLL.	distance between collisions (feet)
HIST. R.N.	random number before start of history
PRES. R.N.	present random number

Stops

Normal

70707 (Pause) end of run at sense switch 4 down, START to rewind output tape, set switch up and START to read new problem data

52525 (Stop) output tape has been rewound - final Stop

Errors

77777 (Pause) redundancy in tape loading, START to proceed, LOAD TAPE to reload tape

700 (Pause) input energy below cutoff. In gamma ray, START to leave as is. For neutron, START to replace by fission source

701 (Pause) number of cases less than one START to replace by one

702 (Pause) number of cavity divisions less than one START to replace by one (gamma ray only)

704 (Pause) input direction negative - see printer for instructions

105 (Stop) mixture set number negative

111 (Stop) cross section negative

112 (Stop) radial division count negative

Appendix 5. Flow Sheets for Monte Carlo Calculations

A. General Flow

B. History - Gamma Ray (Schematic)

C. History - Neutron (Schematic)

D. History - Gamma

E. History - Neutron

F. Geometry Subroutine

G. Symbol Tables for Flow Sheets

A. GENERAL FLOW

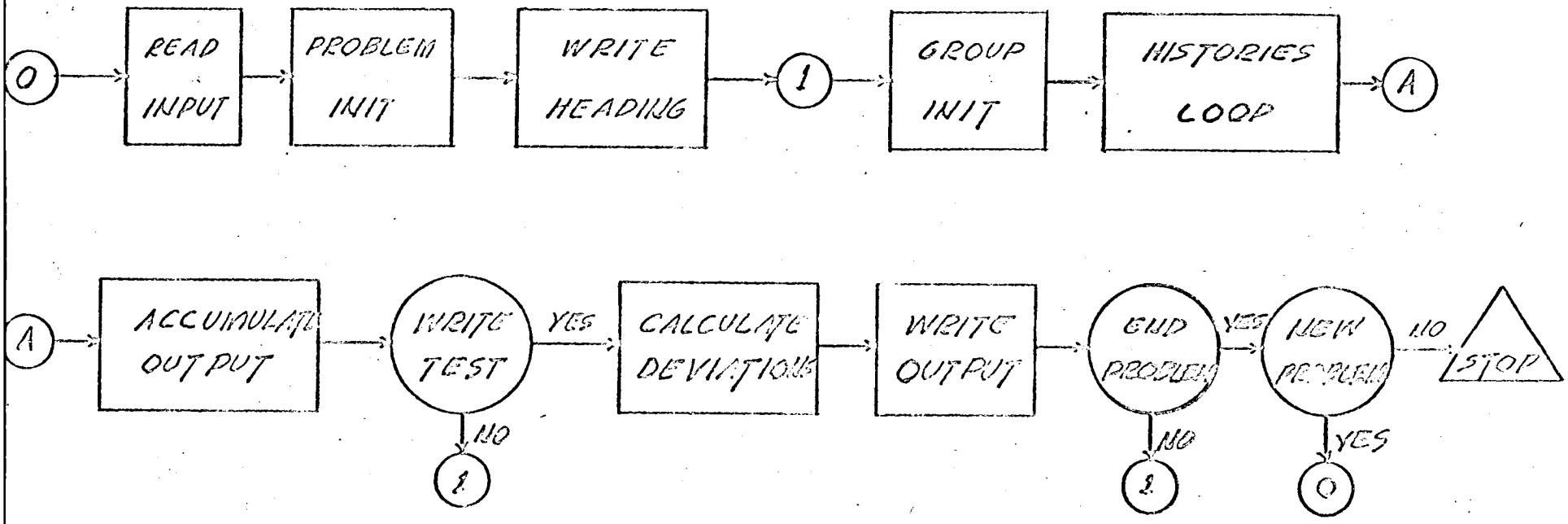

B. HISTORY- GAMMA RAY (SCHEMATIC)

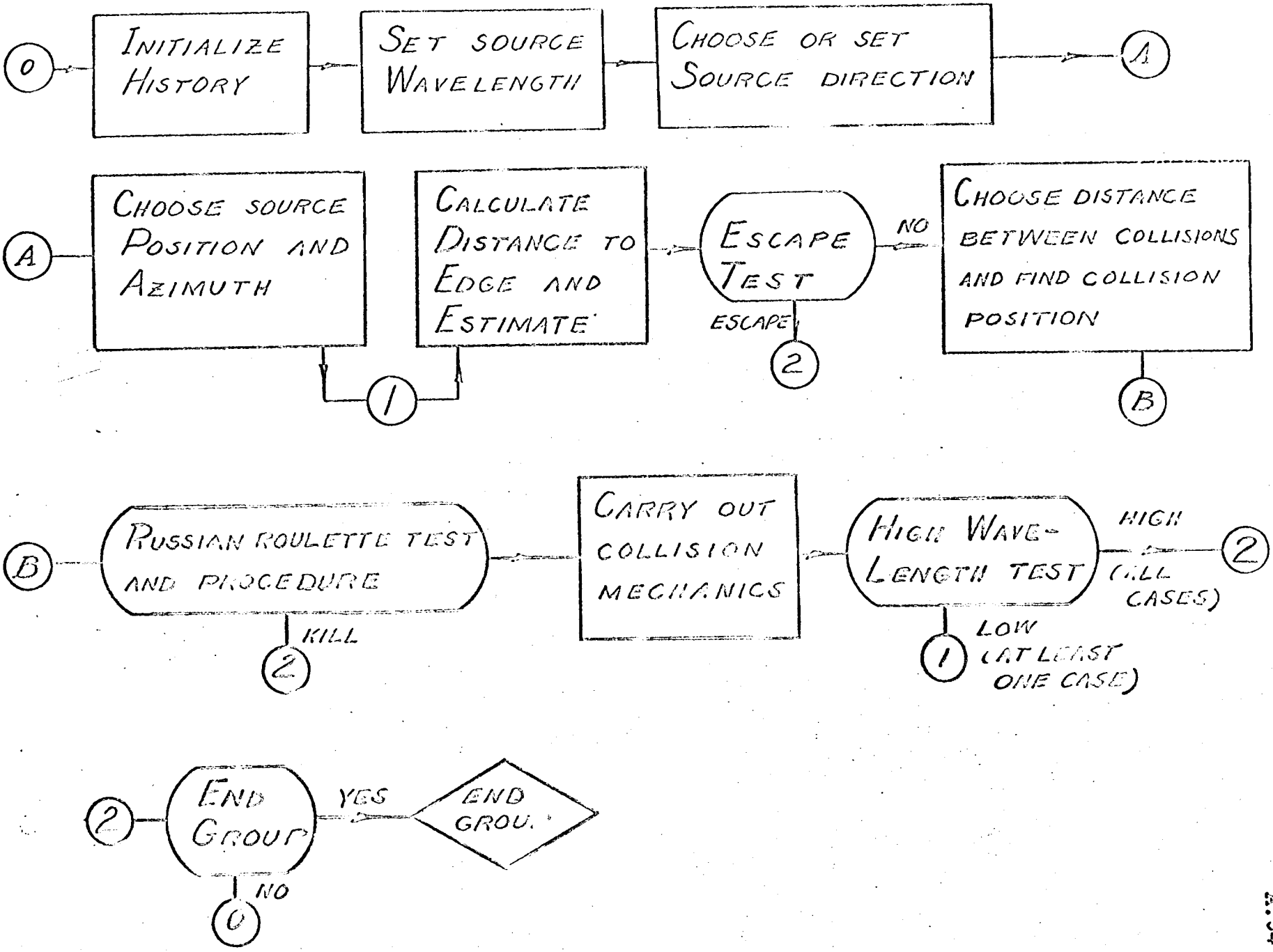

c. HISTORY – NEUTRON (SCHEMATIC)

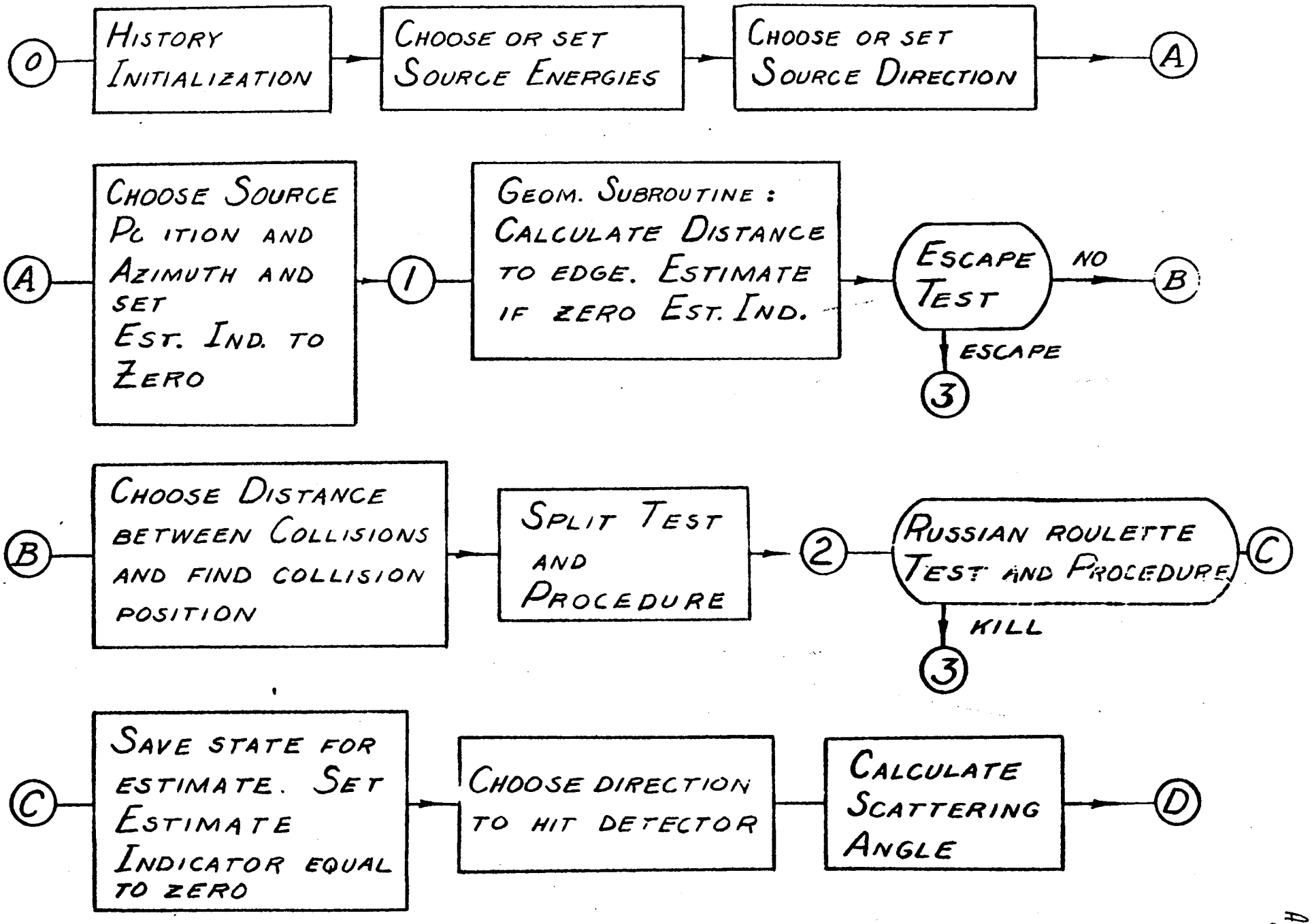

A.C5

C. HISTORY - NEUTRON . (SCHEMATIC)

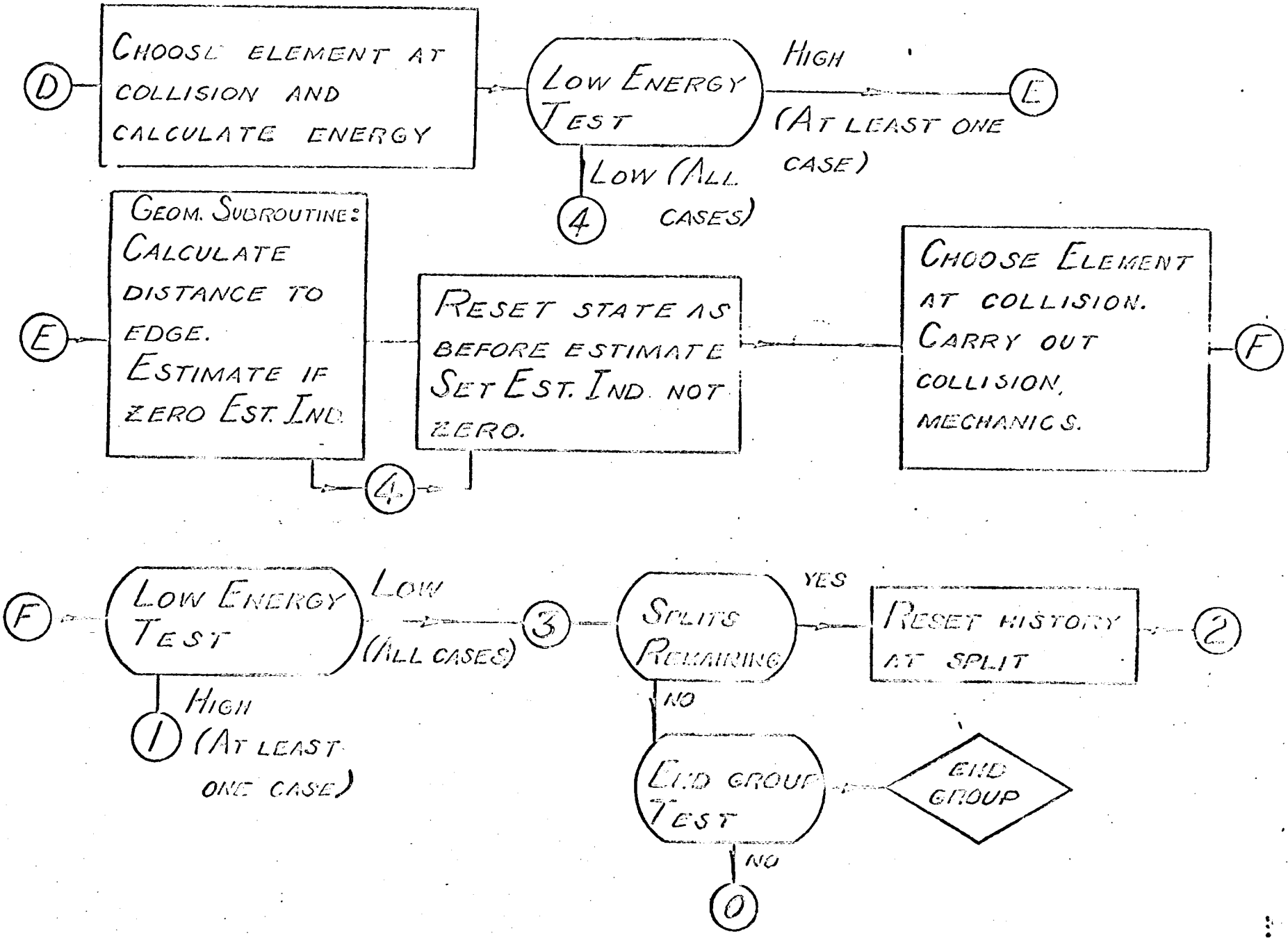

HISTORY – GAMMA

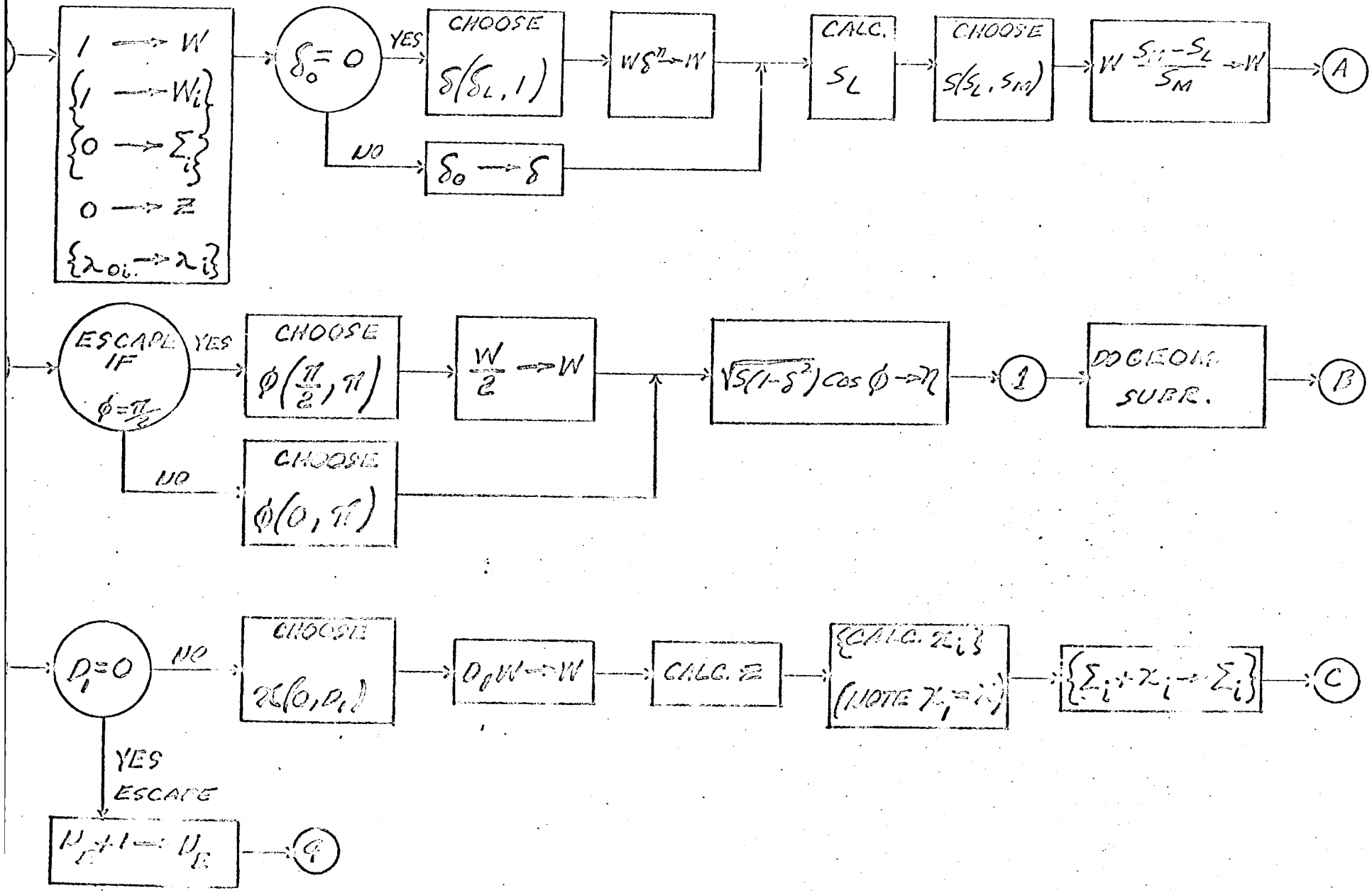

HISTORY = GAMMA

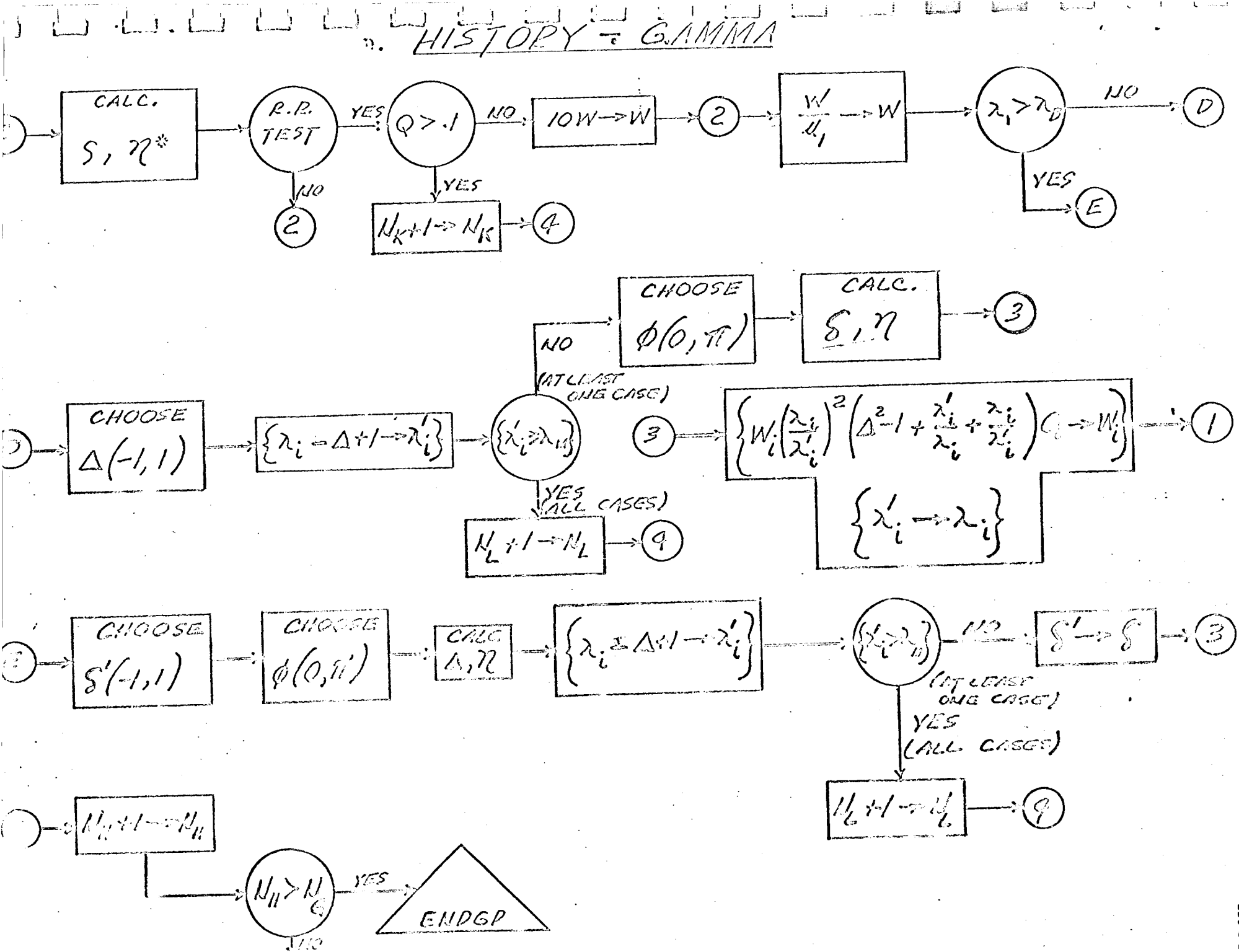

A.60

B. HISTORY — NEUTRON

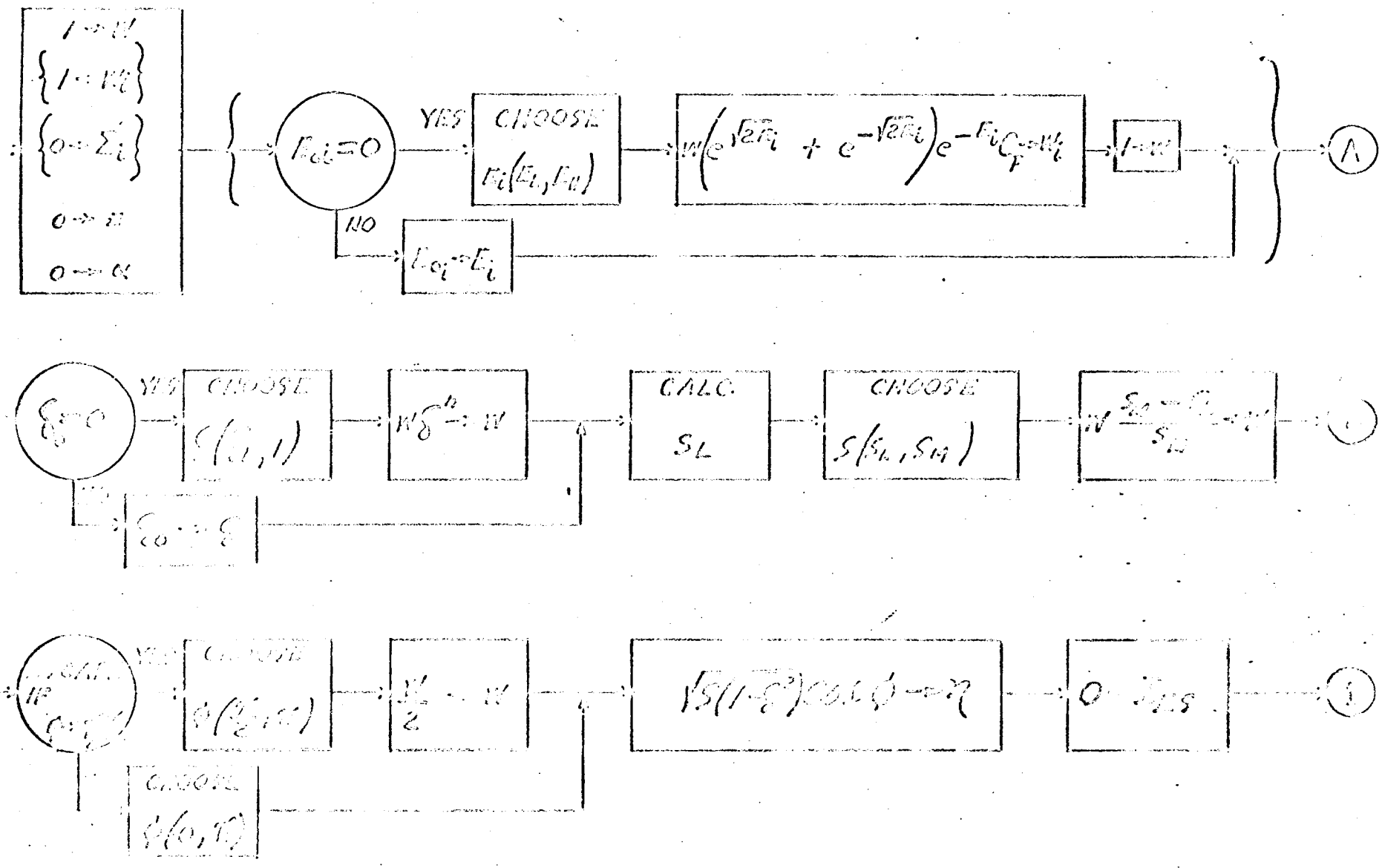

E. HISTORY—NEUTRON (Continued)

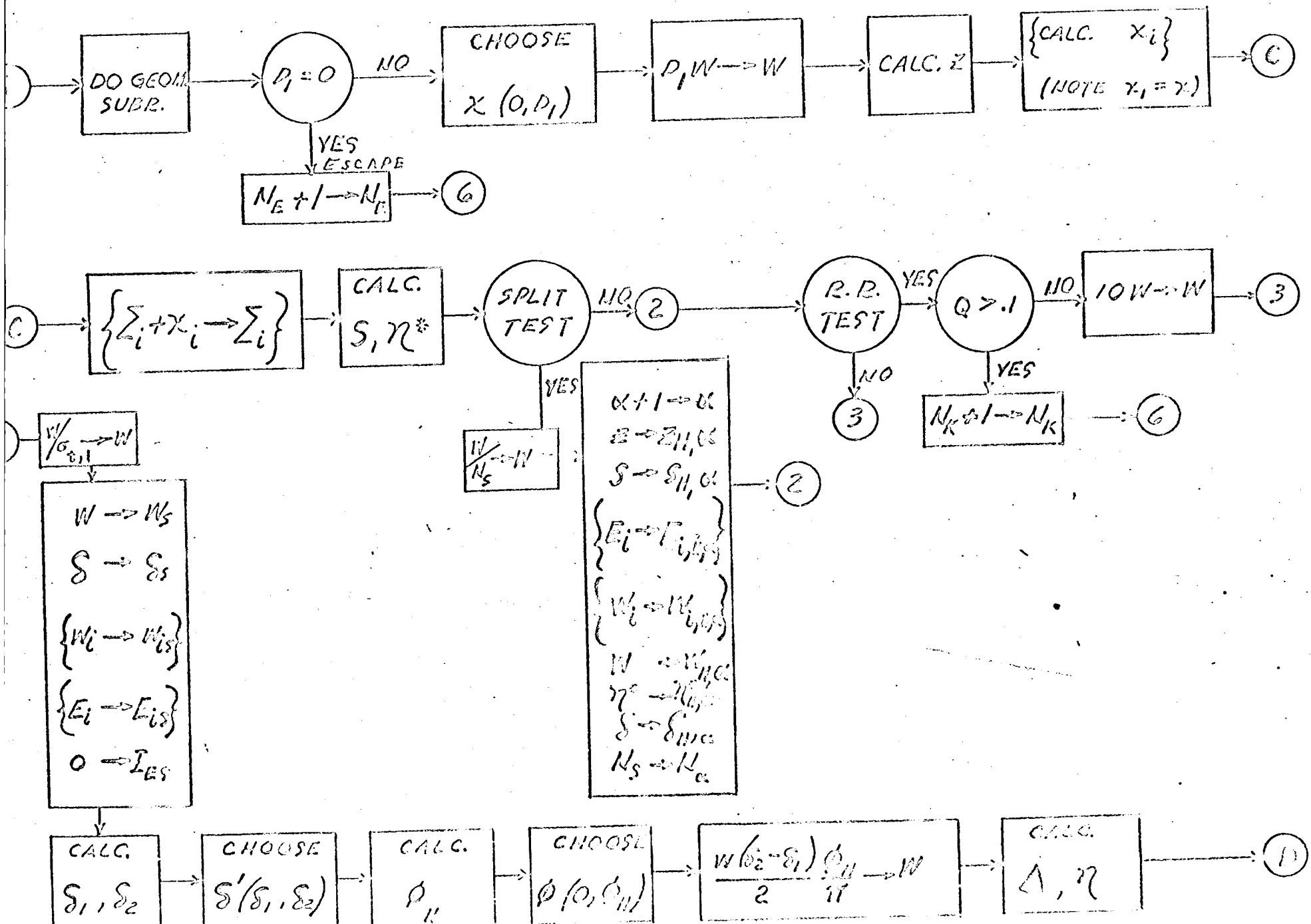

E. HISTORY -- NEUTRON (Continued)

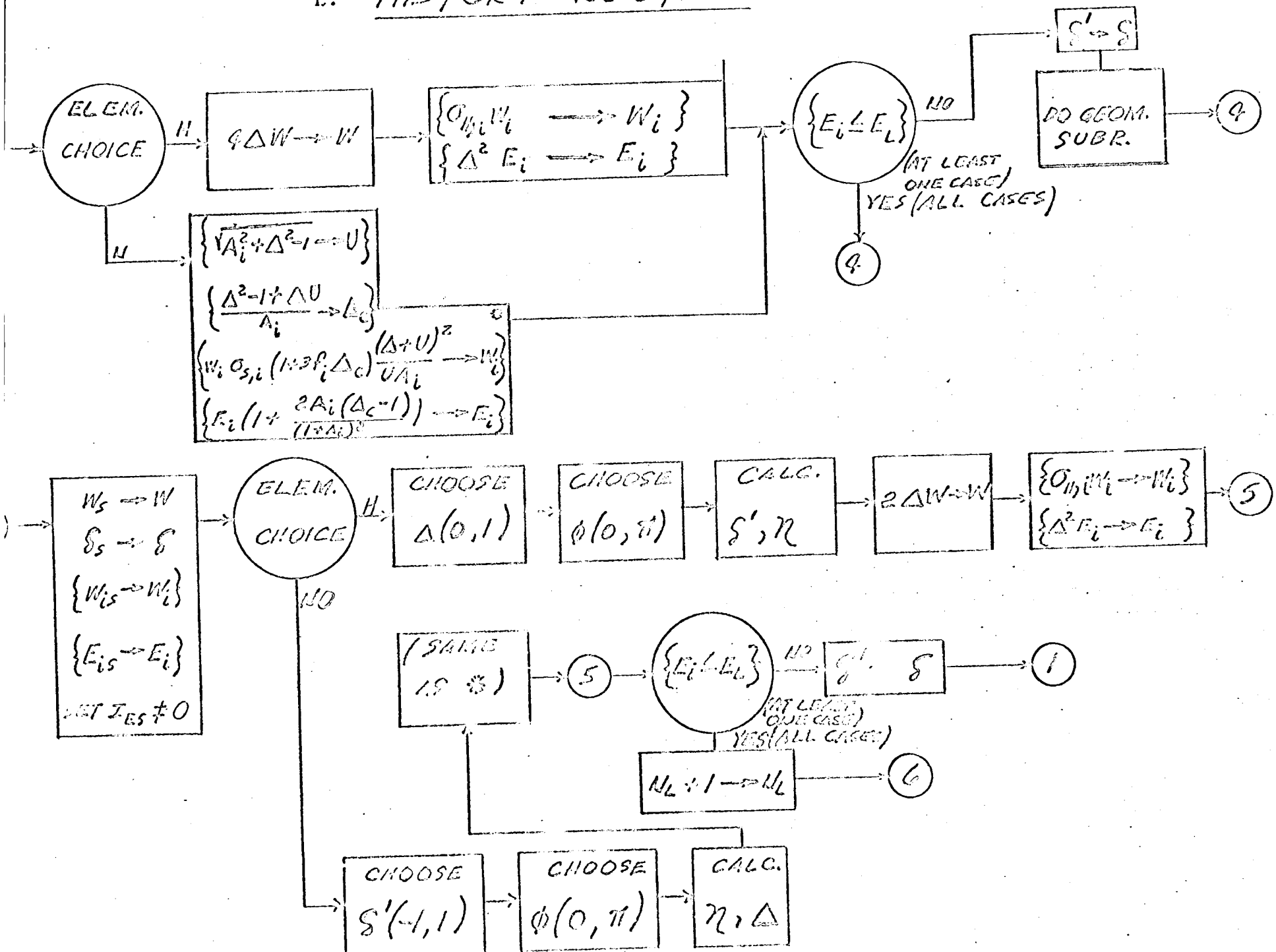

E. HISTORY - NEUTRON (Continued)

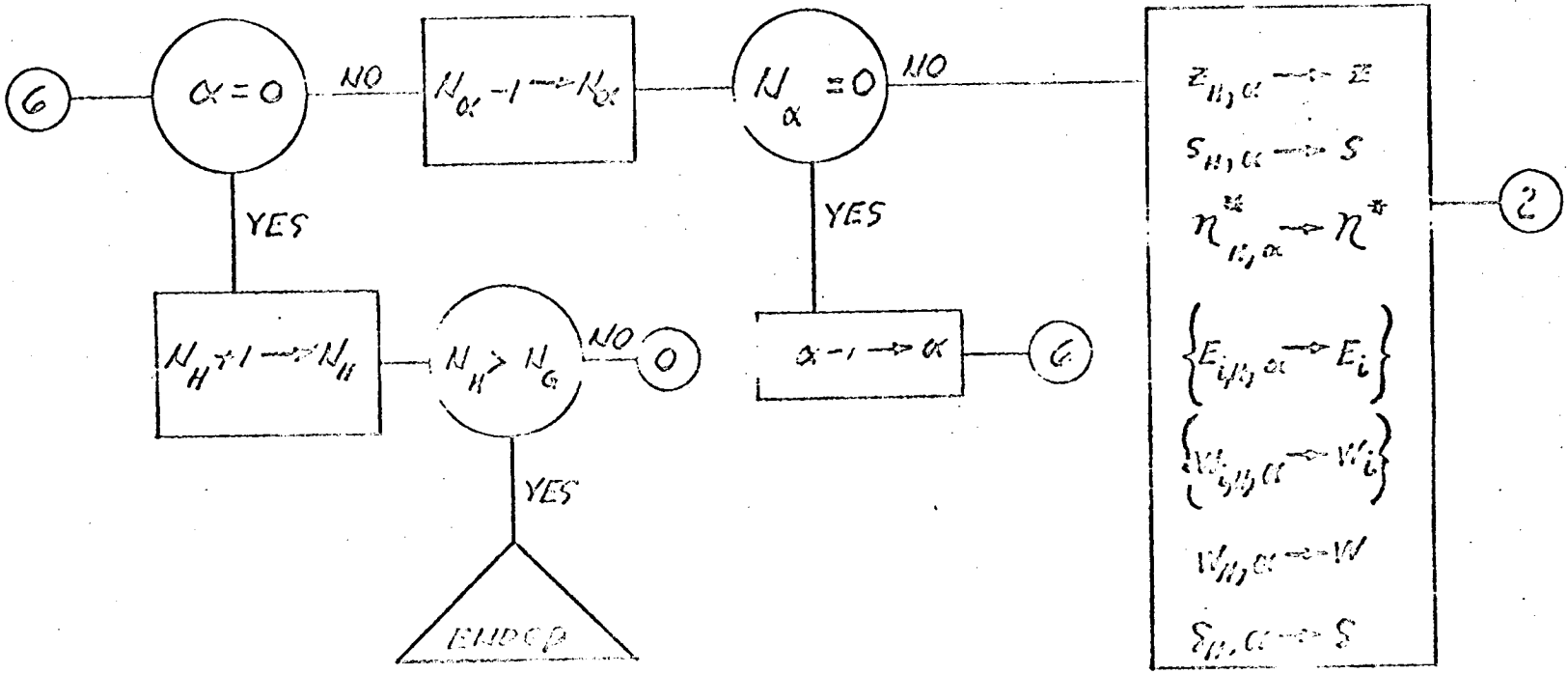

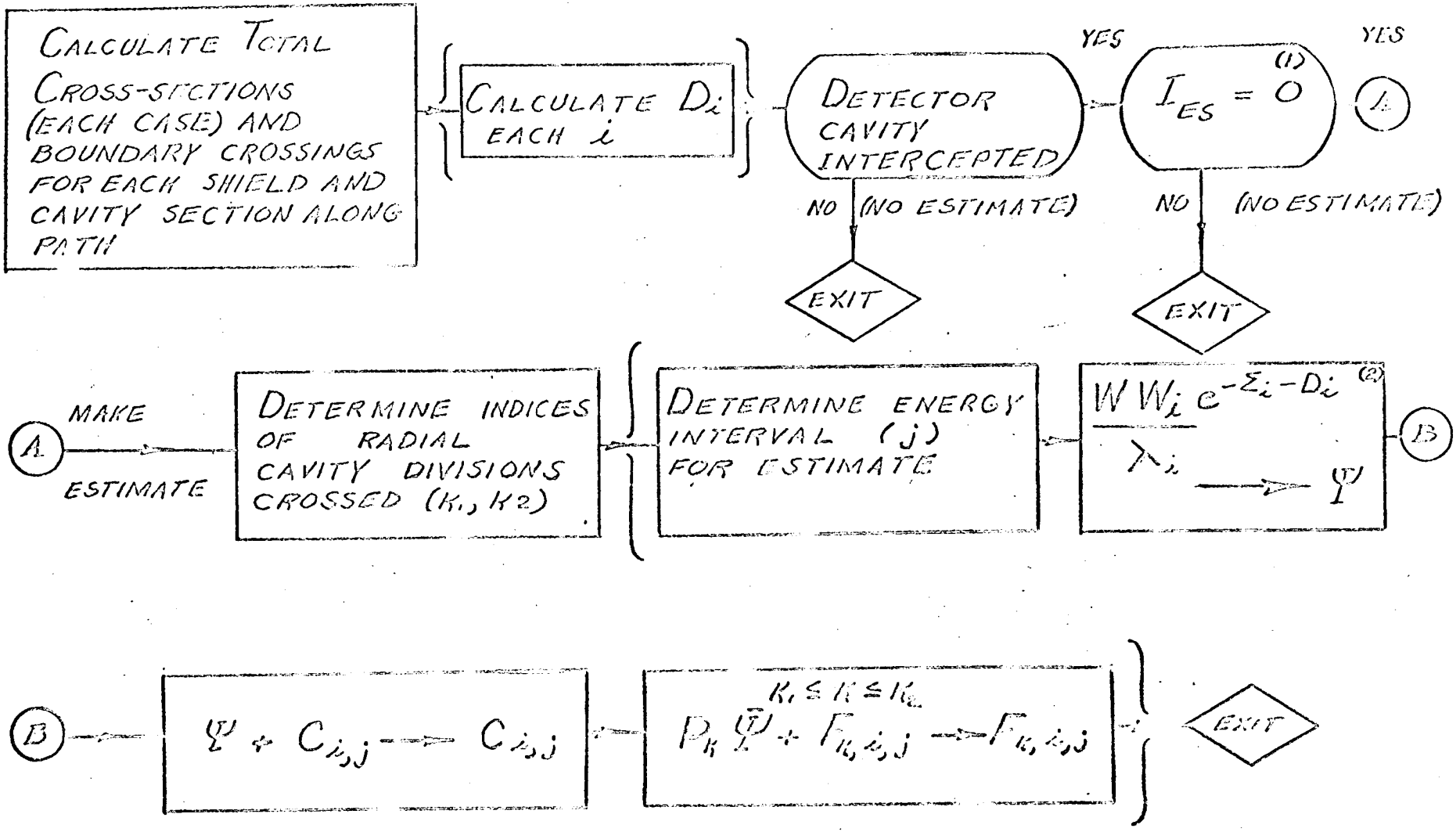

NOTE: (1) I_{ES} TEST PRESENT ONLY FOR NEUTRONS

(2) DIVISION BY λ_i ONLY FOR GAMMA RAYS

G. Symbol Table for Flow Sheets (Neutron & Gamma Rays)

W	fixed weight
W_i	case weight
δ_o	initial cosine of angle with axis
δ	cosine of angle with axis
δ'	cosine of angle with axis after scatter
δ_L	minimum possible initial cosine
n (for δ^n)	prescribed power of initial cosine distribution
η	distance from axis times cosine of angle with radius (at source or after collision)
η^*	distance from axis times cosine of angle with radius (before collision)
ϕ	azimuthal angle
Δ	cosine of scattering angle
S_L	minimum possible source radius squared, for chosen δ_o
S_M	source disk radius squared
S	square of distance from axis
Z	axial position - distance from source disk
Σ_i	total mean free paths travelled - for case i
D_i	mean free path distance to edge for case i
x_i	mean free path distance between successive collisions for case i
N_E	number of histories terminated by error
N_K	number of histories terminated by Russian Roulette
N_L	number of histories terminated by low energy
Q	random number
N_H	history number within group
N_G	number of histories per group

Symbol Table for Flow Sheet

(Gamma rays only)

λ_{oi}	initial wavelength - each case
λ_i	wavelength - each case
λ_i'	wavelength after scatter - each case
λ_B	breakpoint wavelength between high-and low-energy sampling
λ_M	maximum wavelength
μ_i	total cross-section of material for each case (macroscopic)
C_i	Klein-Nishina normalization factor

Symbol Table for Flow Sheets

(Neutrons only)

α index of split order

E_{oi} initial energy - for case i

E_L cutoff energy

E_H maximum energy in fission spectrum

E_i energy - for case i

I_{ES} estimate indicator

$\sigma_{t,i}$ total cross section - for case i (macroscopic)

$\sigma_{H,i}$ hydrogen cross section - for case i (macroscopic)

$\sigma_{S,i}$ non-hydrogen scattering cross section - for case i (macroscopic

f_i first Legendre coefficient of differential cross section - for case i

δ_1 minimum cosine with axis for detector intercept (for estimate procedure)

δ_2 maximum cosine with axis for detector intercept (for estimate procedure)

ϕ_H maximum azimuthal angle for detector intercept (for estimate procedure)

A_i atomic weight of non-hydrogen element - for case i

Δ_c cosine of center-of-mass scattering angle

N_S number of branches at split

C_F fission spectrum normalizing factor

Quantities subscripted H,α or α stored at split

Quantities subscripted S stored for estimate

Additional Symbols for Geometry Subroutine

K_1, K_2	indices of first and last (counted from axis) cavity divisions crossed by extended particle path
ψ	statistical estimate
$C_{i,j}$	accumulated current
$F_{k,i,j}$	accumulated flux
P_k	path length in cavity division k of extended particle path
j	index of energy interval for energy spectrum accumulation

References

1. Klahr, C. N. and Held, K., "Nuclear Shielding for Space Environment - The Scattering Shield" XDC-6-70 Papers from Seventh Semiannual Shielding Information Meeting, October 1959

2. Klahr, C. N. and Held, K., "Some Principles of Nuclear Shadow Shielding" TRG TR-1001, June 1959

3. J. Walsh, Proc. Phys. Soc. XXXII, page 59 (1920)

4. Aronson, R. et al:"Penetration of Neutrons from a Point Isotropic Fission Source in Water, NYO-6267 (1954)

5. Goldstein, H: Private Communication (1960)

6. Grodstein, G. W. "X-ray Attenuation Coefficients from 10 Kev to 100 MEV" NBS Circular 583 (1957)

7. Kalos, M. and Goldstein, H. "Neutron Cross Section Data for Carbon" NDA 12-16 (1956)

8. Steinberg, H. and Aronson, R. "Monte Carlo Calculations of Gamma Ray Penetration" WADC TR 59-771 (1960)

9. Troubetskoy,E. S. "Fast Neutron Cross Sections of Iron, Silicon, Aluminum and Oxygen" NDA 2111-3, Vol. C. (1959)